Spring 2018

Investigations of the Putative AI-2 Receptor Protein LsrB from Thermobacillus composti and Truncations of the Salmonella enterica ser. Typhimurium LsrE Protein

Nicholas E. Petty , '18

Investigations of the Putative AI-2 Receptor Protein LsrB from *Thermobacillus composti* and Truncations of the *Salmonella enterica* ser. *Typhimurium* LsrE Protein

Nicholas E. Petty
Senior Honors Thesis, May 2018
Department of Chemistry and Biochemistry
Swarthmore College, Swarthmore, PA
Advisor: Stephen T. Miller

Table of Contents

Abstract

Bacteria were believed to exist as solitary, unicellular organisms until about 50 years ago with the discovery of quorum sensing by John Woodland Hastings. Since then, numerous studies have examined the broad reaching functions controlled by bacterial quorum sensing, including biofilm formation and virulence. Work done by the Bassler laboratory proposed a "universal" quorum sensing pathway that uses a novel signal molecule, autoinducer-2 (AI-2), for intraspecies and interspecies communication. This quorum sensing pathway uses proteins encoded by the *lsr* operon to uptake and process the AI-2 signaling molecule. This work examines two of these proteins, LsrE and LsrB. LsrE, a putative epimerase, is the final protein in the AI-2 quorum sensing pathway yet to be characterized. Prior attempts at functionality determination through bioassays and crystallographic analysis were unsuccessful. Work herein focused on creating truncations of putatively disordered terminal regions to increase protein stability. In addition to LsrE, this work also focused on the putative AI-2 receptor protein LsrB from *T. composti*. Prior work with *T. composti* LsrB experienced difficulties in functionality assays and crystallographic studies. Here, AI-2 binding is demonstrated using a bioluminescence assay. Binding was further characterized using isothermal titration calorimetry. Finally, an N-terminal truncation of *T. composti* LsrB was generated to facilitate crystallographic studies to determine structure and binding interactions.

Ch. 1 Introduction

Bacteria have long been treated as single cellular organisms, entirely disconnected from their surrounding environment. However, work conducted in the 1970's by John Woodland Hastings at Harvard University demonstrated that bacteria communicate in a manner similar to multicellular organisms.[1] Furthermore, recent work has further gone on to show that this intercellular signaling can occur not just within species, but also between species.[2] This necessarily transforms the way we understand the microbial world, transforming it into a coordinated system of billions of individual bacteria interacting with each other to facilitate dynamic responses to environmental stressors.

Quorum sensing first garnered attention through the study of coordinated bioluminescence. Specifically, early research focused on the symbiosis between the Hawaiian bobtail squid, *Euprymna scolopes*, with the bacterium *Vibrio fischeri* (Figure 1.1)[3] The *V. fischeri* grow until they reach a high enough cell density in the evening, causing bioluminescence. This bioluminescence allows the *E. scolopes* to mimic the moonlight shining into the ocean, hiding it from predators on the ocean floor. Once the *E. scolopes* has survived the night, it expels the *V. fischeri* from its system, dropping their biomass enough that bioluminescence ceases.

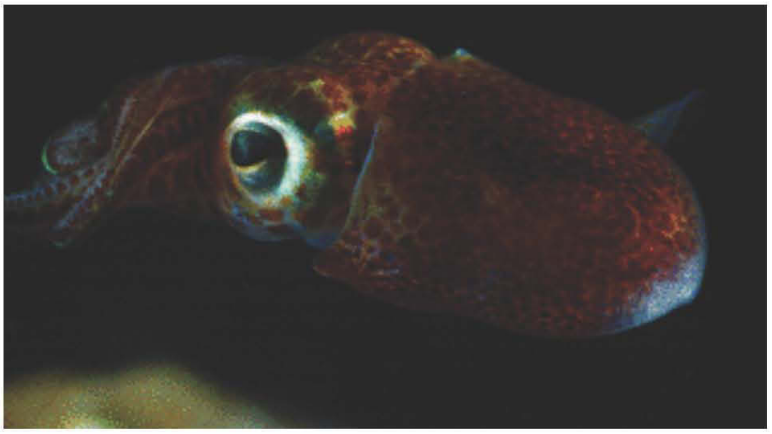

Figure 1.1 *Eupryma scolopes*, the organism in which coordinated bacterial bioluminescence was first observed with *Vibrio harveyi*. Figure adapted from reference 3.

Prompted by this functional symbiosis, further research focused on *V. fischeri* with an emphasis on the mechanisms driving bioluminescence. Work done at the Scripps Institute of Oceanography by the Silverman laboratory discovered that this density dependent bioluminescence was caused by proteins encoded by the *lux* operon.[4] They observed the production of an autoinducer signal molecule by luxI that blocked the repressor molecule encoded by *lux*R. Once LuxR activity is blocked, expression of the rest of the *lux* operon allows bioluminescence to occur. Specifically, the proteins encoded by *lux*A and *lux*B form the α and β subunits of luciferase. Luciferase then catalyzes the oxidation of a reduced flavin and a long chain aldehyde, generated by the LuxCDE complex, producing the bioluminescent effect.[5] Work done by the Greenburg laboratory at Cornell University showed that the ambient concentrations of *V. fischeri* in the ocean (10^2 cells/mL) was not enough to induce bioluminescence, while concentrations found within the light organ of *E. scolopes* (10^{10}-10^{11} cells/mL) did stimulate bioluminescence.[6,7] These data helped establish the density dependent nature of quorum sensing in *V. fischeri.*

While intraspecies quorum sensing was first observed and studied in the context of *V. fischeri*, it has since been expanded to include a wide host of different bacteria and with varying functions. Through a system very similar to that previously described in *V. fischeri*, a signaling molecule known as autoinducer-2 (AI-2) can induce bioluminescence in *Vibrio harveyi*, a close relative of *V. fischeri.*[2,8] Variations of the AI-2 signaling pathway has since been observed in a plethora of other bacteria, leading to AI-2 gaining the colloquial title of the "universal" signaling molecule.[9,10] The AI-2 signaling pathway has also been implicated in a variety of biologically relevant processes that make it of

particular interest, including biofilm formation and virulence expression, in many notable bacterial strains (Table 1.1).[11–18] Better understanding of the underlying mechanisms controlling AI-2 quorum sensing may allow future work to focus on functionalizing this pathway.

Table 1.1 Partial list of notable bacteria that participate in AI-2 quorum sensing. Adapted from reference 41.

Classification	Species
Gram-Positive Bacteria	*B. subtilis, B. antracis, B. halodurans, B. burgdorferi, C. botulinum, C. perfringens, C. difficile, E. faecalis, L. monocytogenes, M. tuberculosis, S. aureus, S. pyogenes, S. pneumonia*
Gram-Negative Bacteria	*H. influenza, N. meningtidies, V. cholera, V. harveyi, E. coli, S. typhimurium, Y. pestis, C. jejnuni, B. antracis, B. subtilis, B. halodurans, S. aureus, L. monocytogenes, H. pylori*

The term AI-2 encompasses multiple cyclized forms of the molecule (4S)-4,5-dihydroxy-2,3-pentadione (DPD). The borated form of AI-2, (2S,4S)-2-methyl-2,3,3,4-tetrahydroxytetrahydrofuranborate (S-THMF-borate), is naturally in *V. harveyi*.

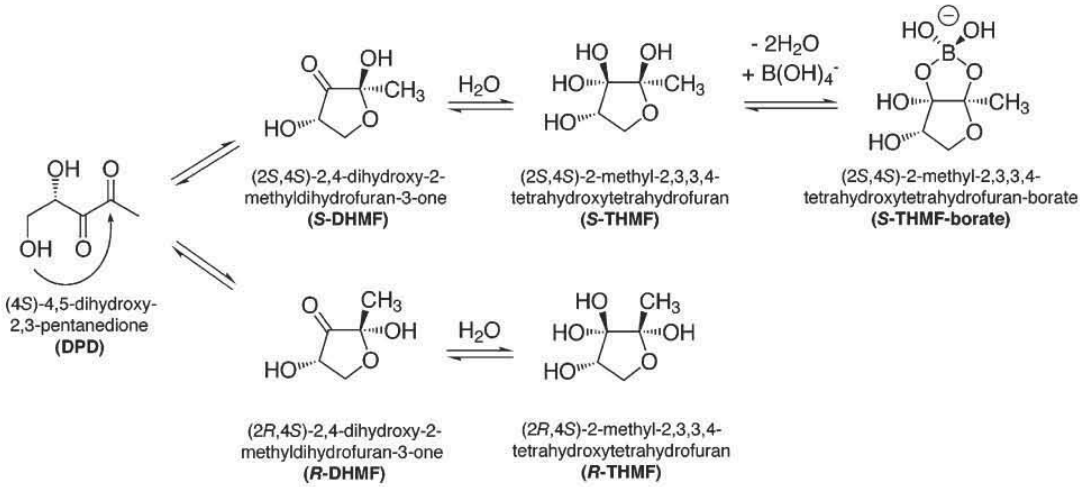

Figure 1.2 The equilibrium between borated (S-THMF-borate) and non-borated (R-THMF) AI-2 molecules. Adapted from reference 10.

More recent work done by the Bassler and Hughson groups at Princeton University has shown that a natural equilibrium exists between the borated form, S-THMF-borate, and a non-borated form, (2R,4S)-2-methyl-2,3,3,4-tetrahydroxytetrahydrofuran (R-THMF).[19] These molecules interconvert by passing through DPD as an intermediate state. This equilibrium further broadens the array of bacteria that use AI-2 quorum sensing (Figure 1.2).

Like LuxI signaling in *V. fischeri*, DPD is produced by the protein LuxS and secreted into the extracellular fluid surrounding the cell.[20] The AI-2 molecule is then imported and processed by a host of proteins produced by the LuxS-regulated (*lsr*) operon. The *lsr* operon contains the genes *lsrACDBFGE*. The genes *lsrR,* and *lsrK* are transcribed separately from the *lsr* operon (Figure 1.3).

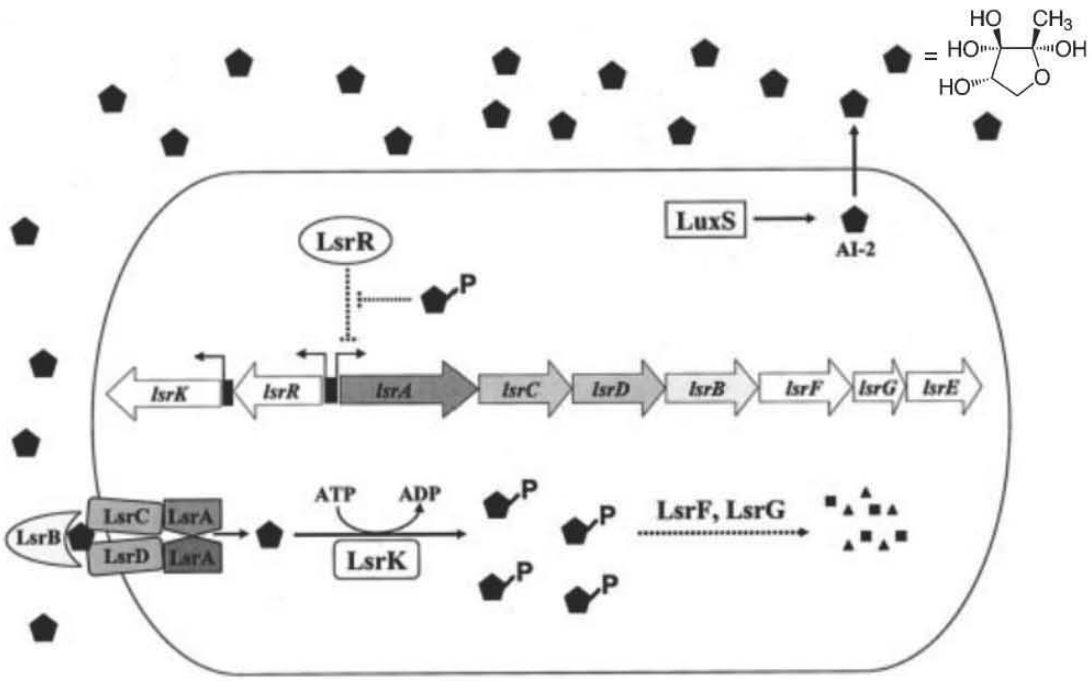

Figure 1.3 A cartoon depicting the AI-2 quorum sensing pathway. This shows the production, uptake, and degradation of AI-2. Adapted from reference 22.

AI-2 is first recognized by LsrB before internalization by the ABC transport cassette composed of LsrA, LsrC, and LsrD.[19,21–23] Once internalized, AI-2 is phosphorylated by LsrK to sequester it inside of the cell. This phosphorylation also generates the activated form of AI-2, phospho-AI-2.[24] Phospho-AI-2 then binds LsrR, the repressor protein for the *lsr* operon, causing de-repression.[23] This allows the cell to take in more AI-2, depleting the environment of AI-2 and generating the desired signal once concentration of internal AI-2 concentration is high enough. Finally, the LsrF and LsrG proteins catalyze the degradation of phospho-AI-2 yielding metabolites acetyl-Coenzyme A and dihydroxyacetone phosphate (DHAP). (Figure 1.4).[25,26]

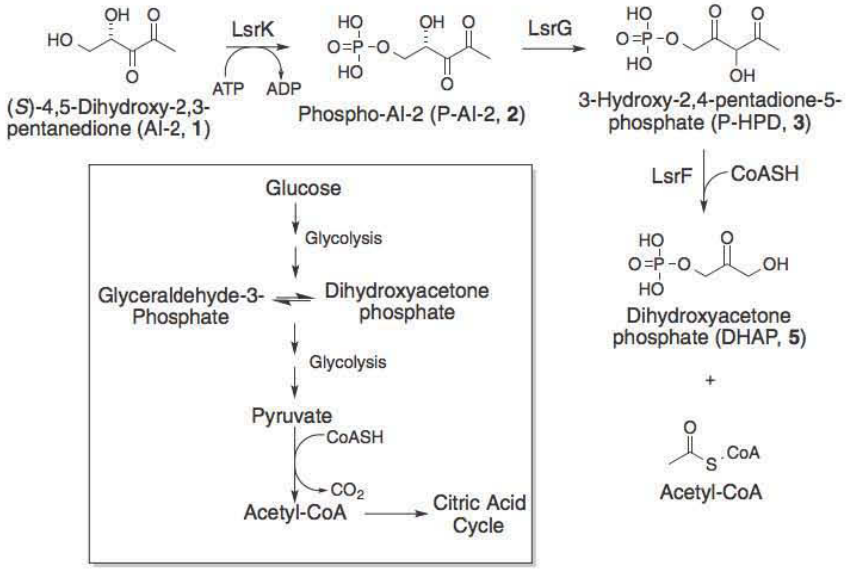

Figure 1.4 The phosphorylation and degradation of the phospho-AI-2 signaling molecule following uptake into the cell. Adapted from reference 24.

LsrE presents an interesting challenging in all of this, as it represents the sole protein coded for by the *lsr* operon that has yet to be characterized. Furthermore, unlike the other Lsr proteins, *lsrE* is only known to be present in the genome of *Salmonella enterica* ser. *Typhimurium*. Additionally, Δ*lsrE* mutants of *S. Typhimurium* show no phenotypic differences from wild type *S. Typhimurium*, leaving the role of LsrE in the

AI-2 quorum sensing pathway unknown.[27] Previous work with LsrE has been unsucessful after facing challenges in production caused by low solubility, making further analysis through assays or crystallization challenging (Audrey Allen, Unpublished Data).

While LsrE has proven to be a challenge, research into the AI-2 receptor protein, LsrB, has been flourishing. Collaboration between the laboratories of Stephen Miller at Swarthmore College and Karina Xavier at the Institute of Chemical and Biological Technology in Oeiras, Portugal has expanded the scope by identifying AI-2 receptors in a range of bacterial species.[27] Sequence analysis using the Kyoto Encyclopedia of Genes and Genomes (KEGG) has afforded an expanded list of AI-2 receptors of varying sequence identities to canonical AI-2 LsrB-type receptors found in *S. Typhimurium*. This has recently allowed characterization of *Clostridium saccharobutylicum* LsrB, which shares only a 30% sequence identity with canonical *S. Typhimurium* LsrB. This distant analog of LsrB has been confirmed to show AI-2 binding through crystal structures and binding assays. Recent work has focused on even less conserved proteins, particularly the putative LsrB protein isolated from the *Thermobacillus composti*, which shares only 17% sequence identity with canonical *S. Typhimurium*.

This study primarily focuses on two proteins within the AI-2 signaling pathway, LsrB and LsrE. With recent work into less conserved LsrB analogs yielding functional LsrB proteins only sharing 30% sequence identity with canonical *S. Typhimurium* LsrB, the less conserved *T. composti* LsrB presents a next step towards testing the limits of what can be identified as a LsrB receptor protein. In addition, this work looks to expand upon past attempts at characterizing the *S. Typhimurium* LsrE protein, whose function remains unknown. A strategy employing both functional analyses through assays along

with structural characterization through X-ray crystallography was employed to expand the body of knowledge concerning these proteins.

Ch. 2 Creation and Purification of LsrE Truncations

BACKGROUND

The LsrE protein is the one protein encoded by the *lsr* operon that has yet to be characterized. This protein is also unique because, unlike the other Lsr proteins, LsrE is only produced naturally by a single bacterial species, *Salmonella enterica* ser. *Typhimurium*. Prior sequence analysis using the Basic Local Allignment Search Tool (BLAST) showed that LsrE has a 37% sequence identity with ribulose-5-phosphate-3-epimerase isolated from *Haemophilus somnus*. Epimerases are a class of enzymes that that catalyze stereocenter inversion reactions[28,29]. Specifically, LsrE closely resembles five carbon sugar epimerases, highlighting the AI-2 molecule as a potential target of stereocenter inversion.

Sam Tanner of the Miller laboratory at Swarthmore College conducted the initial work on LsrE. Tanner cloned the full length LsrE protein as an N-terminal fusion with maltose binding protein (MBP) to enhance solubility, into *Escherichia coli* expression vectors, validated the subsequent purification procedure to obtain pure LsrE, and began initial crystallization attempts.[30] At this stage, the Miller group's LsrE project was passed on to Audrey Allen, who looked to further the functional and structural work into LsrE through functionality assays and crystallization. The functionality assays carried out by Allen focused on the potential epimerase activity of LsrE; specifically focusing on whether LsrE could racimize stereocenters on AI-2 or its analogs. She measured the rate of LsrF/LsrG catalyzed phospho-AI-2 degradation with and without LsrE present using a nicotinamide adenine dinucleotide (NADH) consumption assay. This assay coupled the production of DAPH with the consumption of NADH using glycerol-3-phosphate

dehydrogenase. NADH consumption was measured by observing absorbance at 340nm (Audrey Allen, Unpublished Data).[31]

While Allen was able to obtain pure protein using the purification procedure validated by Tanner, problems quickly arose concerning the utility of the LsrE protein. Specifically, the LsrE protein exhibited limited solubility following removal of the MBP tag. This instability caused the protein to precipitate before analysis through the NADH consumption assay or crystallization.

One easy target for modification that could promote solubility without compromising protein functionality comes from removal of inherently disordered regions. The present chapter presents attempts to create mixed N- and C-terminal truncations of various lengths to LsrE with the intention of promoting the solubility of the LsrE protein following removal of the MBP solubility tag.[32]

MATERIALS AND METHODS

Creation of LsrE truncations

N- and C-terminal disordered regions of varying length were predicted using Protein Homology/analogy Recognition Engine V2.0 (PHYRE^2) prior to truncation efforts (Figure 2.1).[33]

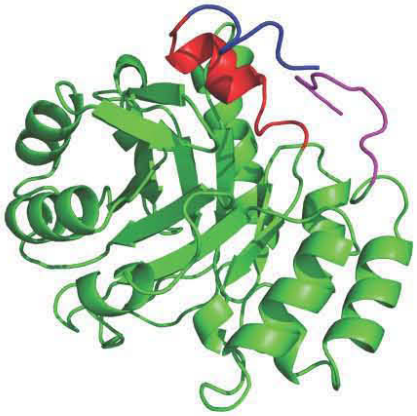

Figure 2.1 *Salmonella Typhimurium* LsrE as modeled by Phyre^2. Blue and red labels correspond to 7' and 19' N-terminal truncated regions respectively. The magenta label corresponds to the 244' C-terminal truncation.

Once identified, primers were ordered from Sigma (Table S1). Truncations were generated by combining two possible N-terminal truncations with one C-terminal truncation, yielding a total of five unique truncation combinations (Table 2.1). Truncations were produced by PCR amplification of *S. Typhimurium* (strain LT2/SGSC1412/ATCC700720) genomic DNA using Pfu Ultra II Fusion HS DNA polymerase (Agilent).

Table 2.1 Construct names for truncations created by combining two N-terminal truncations and one C-terminal truncation.

Truncation Name	Forward Primer	Reverse Primer
LsrE 1	LsrE 7' Truncated Forward	LsrE Non-Truncated Reverse
LsrE 2	LsrE 7' Truncated Forward	LsrE 244' Truncated Reverse
LsrE 3	LsrE 19' Truncated Forward	LsrE Non-Truncated Reverse
LsrE 4	LsrE 19' Truncated Forward	LsrE 244' Truncated Reverse
LsrE 5	LsrE Non-truncated Forward	LsrE 244' Truncated Reverse

Cloning of His-MBP-LsrE Truncations

Once the truncations were generated, PCR purification was performed using the QIAquick PCR Purification Kit (QIAGEN) before cloning into the pENTR/TEV/D-TOPO vector (Invitrogen). The LsrE truncations in the pENTR vector were then transformed into One Shot TOP10 Chemically Competent *E. coli* (Invitrogen) for plasmid overexpression. Plasmid from the One Shot cells was purified using a QIAprep Spin Miniprep Kit (QIAGEN). Cloning success was assessed by PCR amplification using the truncated *lsrE* primers and Taq DNA polymerase (NEB).

The *LsrE* truncations in the pENTR vector were then transferred into the pDEST/His_6/MBP vector (Addgene) using Gateway LR clonase (Invitrogen).[34] The pDEST/pENTR/LsrE fusions were then transformed into One Shot cells for plasmid overexpression. Plasmids were again purified and visualized as before, and sequence was

verified using Sanger sequencing (Genewiz). Plasmid with insert identity verified was transformed into Ca^{2+} competent BL21 (DE3) cells for protein expression.

Growth and Expression of LsrE/His/MBP

BL21 (DE3) *E. coli* carrying the pENTR/pDEST/LsrE plasmid were grown overnight at 37°C as 100mL LB Miller (Difco) liquid cultures with 100µL of 100mg/mL ampicillin (VWR). One-liter flasks with 1mL of 100mg/mL ampicillin were inoculated using 10mL of the prepared overnight cultures and allowed to grow at 37°C for two hours while shaking. When the optical density at a wavelength of 595nm (OD_{595}) had reached 0.5, the temperature was dropped to 22°C and the cells were allowed to grow for approximately another hour. When the OD_{595} had reached 1.0, each 1L culture was induced with 100µL of 1M isopropyl-β-D-1-thiogalactopyranoside (IPTG, CalBioChem) and allowed to express for eight hours. Following this expression period, cells were centrifuged in 750mL centrifuge tubes (Nalgene) for 10 minutes and resuspended in 20mL supernatant to increase cell density. A final centrifugation in 50mL Falcon tubes for 30 minutes yielded ~5mL pellets. Supernatant was decanted and pellets were stored at -80°C.

Purification LsrE/His/MBP

Protein pellets were thawed on ice and suspended by vortexing in 20mL of lysis buffer (50mM sodium phosphate (Sigma), 300mM sodium chloride (JT Baker), 10mM imidazole (JT Baker), 1.4mM β-mercaptoethanol (Sigma), pH 8.0). Once re-suspended, 10µg/mL DNase (AlfaAesar) and 10µg/mL leupeptin (CalBioChem) were added to the cell buffer solutions. Cells were then passed through a M-110Y microfluidizer (Microfluidics) for lysis. Lysate was centrifuged at 18,000 RPM to remove cellular debris and supernatant was decanted from the cellular debris immediately following

centrifugation. Supernatant was then passed over Ni-nitrilotriacetic acid (NTA) columns prepared with 4mL of 50% Ni-NTA agarose solution (Qiagen) to give a final bed volume of 2mL. Nickel columns were pre-equilibrated in lysis buffer. When all supernatant had passed over three Ni-NTA columns in series, each column was washed with three installments of 5mL of wash buffer (50mM sodium phosphate, 300mM sodium chloride, 20mM imidazole, 1.4mM β-mercaptoethanol, pH 8.0). Protein was then eluted by 2mL additions of elution buffer (50mM sodium phosphate, 300mM sodium chloride, 250mM imidazole, 1.4mM β-mercaptoethanol, pH 8.0) repeated four times. Preliminary protein yields were determined using the ND-1000 spectrophotometer (NanoDrop) absorbance at 280nm (A_{280}), and purity was assessed by SDS-PAGE. Protein characterstics were calculated using the ProtParam software (ExPASy, Table S2).[35]

After initial purification over the Ni-NTA columns, His-MBP-LsrE was exchanged into lysis buffer using the HiPrep desalting column. Following the initial buffer exchange, tobacco etch virus (TEV) protease was added in a 1:15 w/w ratio to LsrE to remove the His-MBP tag. After overnight incubation at 4°C, Ni-NTA columns were run as outlined previously and protein was identified by A_{280}. The non-tagged LsrE was then transferred to an ion exchange buffer (25mM Tris, 150mM sodium chloride, 1mM 1,4-dithiothreitol (DTT), pH 8.0) before further purification.

After TEV protease digestion and buffer exchange, further purification was carried out using the Source15Q anion exchange column (GE Life Sciences). Purification was carried out in buffer A (25mM Tris, 1mM DTT, pH 8.0), increasing sodium chloride concentration from 150mM to 1000mM over 20 column volumes. Collected fractions were assessed for purity and protein content using SDS-PAGE. Selected fractions were pooled and concentrated to a final volume under 5mL. Final purification was performed

with the Superdex 75 or Superdex 200 size exclusion chromatography (SEC) columns (GE Life Sciences), yielding pure protein in the ion exchange buffer.

RESULTS

Purification of LsrE Truncations

Initial trials of purification demonstrated that all truncations showed low solubility. Of the five truncations generated, only the C-terminal truncation showed any significant portion of expressed protein in the supernatant following lysis and centrifugation (Figure 2.2).

Figure 2.2 Overexpression of LsrE Truncation 5 yielded soluble protein while other truncations did not. This gel shows initial purification by nickel column for three LsrE truncations: 1, 4, and 5.

Further purification efforts were concentrated on this truncation. Separation via Ni-NTA columns was successful and initial protein yields were acceptable.

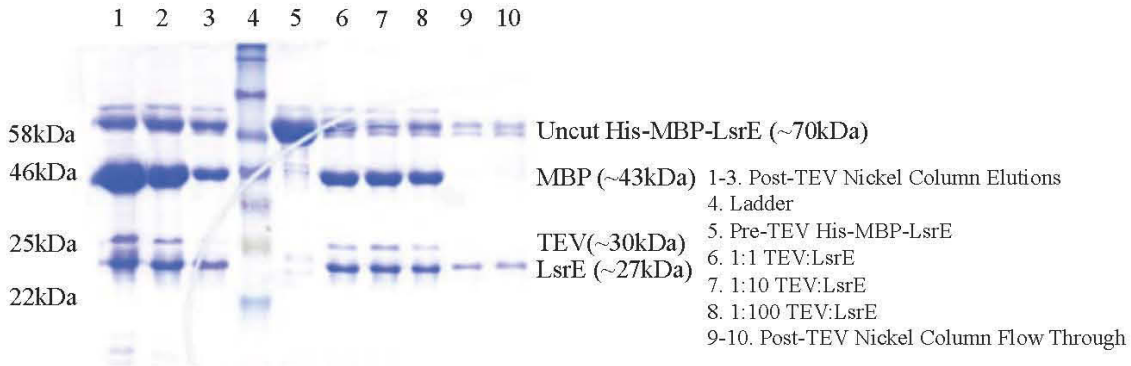

Figure 2.3 TEV protease cleaved His-MBP-LsrE 5 even at low concentrations. However, subsequent purification using nickel columns did not prove useful with both the tagged and non-tagged protein sticking to the column until elution.

TEV protease demonstrated appreciable cutting of the His-MBP tag even at low concentrations (Figure 2.3). Further problems arose when trying to separate cleaved and uncleaved protein using Ni-NTA columns. The truncated *S. Typhimurium* LsrE showed binding to the Ni-NTA columns without the His-MBP tag, rendering this separation step useless. Separation of the His-MBP tag and the LsrE truncation was successfully carried out on the Source15Q anion exchange column, but no separation was observed between the LsrE with and without His-MBP tag (Figure 2.4).

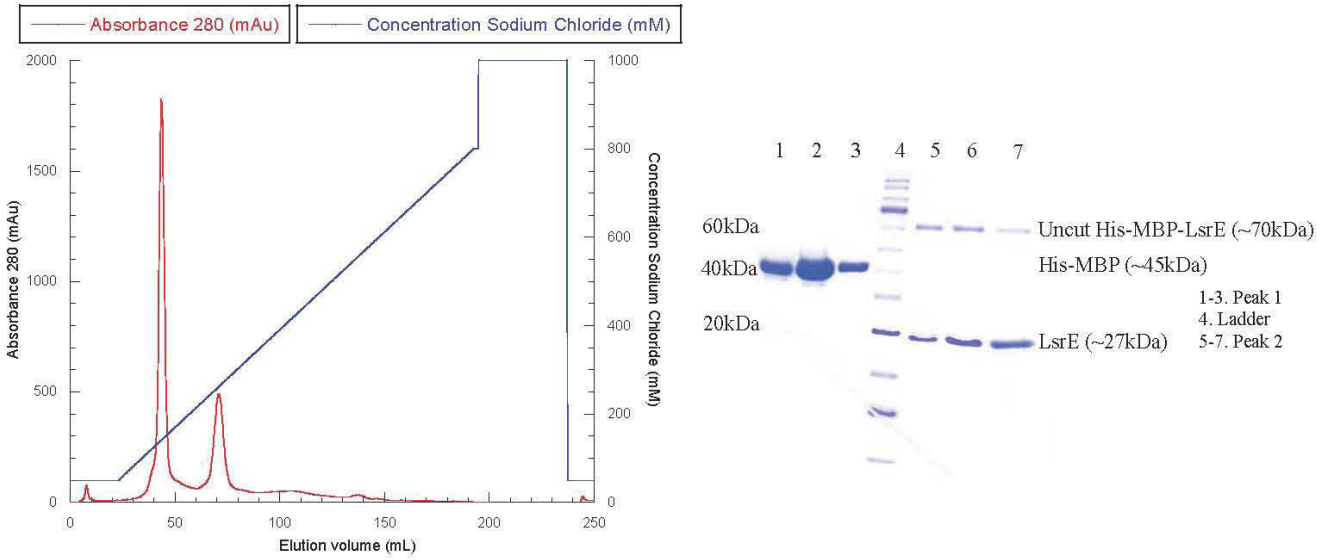

Figure 2.4 SourceQ ion exchange at pH 8.0 successfully separated MBP from LsrE, but failed to separate LsrE with and without the His-MBP tag. MBP eluted at 150mM sodium chloride, while LsrE with and without tag eluted at 300mM sodium chloride.

Further purification steps carried out with the Superdex 75 showed no separation, but separation of the His-MBP-LsrE fusion on the Superdex 200 SEC (GE Life Sciences) showed separation of three distinct peaks.[36] Comparison to the standard solution showed the largest peak corresponded to molecular weights of 120kDa, approximately double the expected monomeric weight for the tagged protein (Figure 2.5). Following these purification steps, another issue arose as protein remained in solution for only a very short time. Even at low concentrations, removal of the His-MBP tag caused LsrE to precipitate, rendering it useless for further crystallization or functional assay attempts.[37]

Figure 2.5 Separation by two size exclusion methods suggested the multimerization of LsrE. LsrE eluted from the S75 10/300 column in the void volume (A), while His-MBP-LsrE eluted off of the S200 16/60 column at 8mL (B). This elution volume corresponds to a molecular weight of approximately 120kDa.

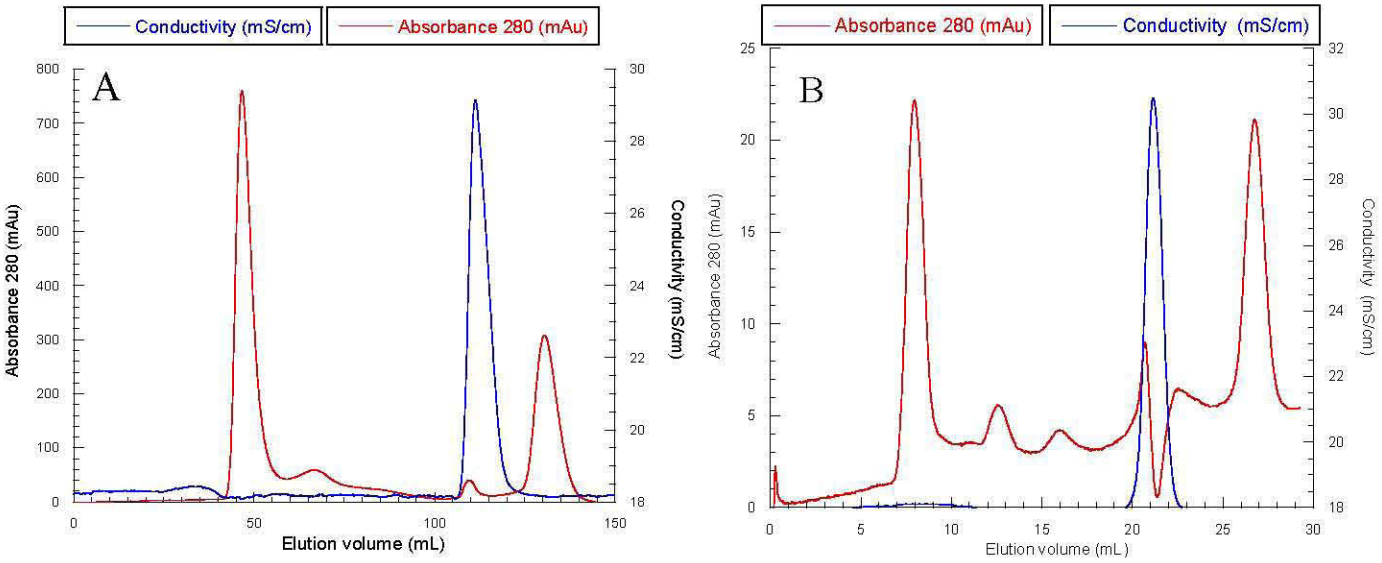

DISCUSSION

This work with LsrE highlights some of the biggest issues that can arise during protein characterization. Overexpressing protein can create an unrealistic environment where protein concentrations are far higher than they are naturally. This can lead to proteins behaving in non-ideal ways and, in this case, precipitation. This result matches closely with the work done on full length LsrE conducted by Audrey Allen and Sam Tanner, who observed similar solubility issues.

While there were no observed solubility enhancements from removing the predicted less ordered N- and C-terminal regions, this does not mark an end into the work with LsrE. Other studies have established that both crystallization and functionality assays can work with solubility tags still attached.[38] These studies suggest that the use of a shorter linking region is desirable, so most likely more DNA work would be required get the LsrE protein and its truncations into an appropriate vector. Another avenue that was only explored briefly in this study was varying the growing conditions to increase protein solubility. Supplementing the LB media with glycerol, lowering the induction temperature, or decreasing IPTG concentration are all potential answers to the problem of initial protein solubility.[32]

Apart from the issues of solubility, this work with LsrE highlights one interesting aspect of LsrE not touched upon before, size. The truncated LsrE protein ran on the S200 at about 120kDa, which is approximately double the expected weight of the monomeric His-MBP-LsrE protein. This suggests that the LsrE protein may be forming a dimer in solution. This would match previous studies that demonstrated that ribulose-5-phosphate-3-epimerase enzymes form homodimers in solution.[28,29] This offers the first promising evidence past structural homology that LsrE may act as a putative epimerase in

S. Typhimurium. There are two experiments that would further probe this potential dimerization of LsrE. The first experiment would simply be to run a native gel. Unlike SDS-PAGE, native gel electrophoresis would allow visualization of any dimers formed by LsrE. Another experiment to assess the epimerase functionality of LsrE could instead focus on the binding interaction between LsrE and its putative substrate. Surface plasmon resonance and isothermal titration calorimetry would both work well in this capacity.[39,40] These kinetic studies could act as an important intermediary step in determining the function of LsrE while crystallization remains out of reach.

Ch. 3 *Thermobacillus composti* LsrB AI-2 Binding Bio-assay

BACKGROUND

In contrast to LsrE, the LsrB receptor protein has seen much more attention and success in both functional and structural characterization. Recent studies done in collaboration between the Miller laboratory of Swarthmore College and the Xavier laboratory of the Institute of Chemical and Biological Technology have expanded the scope of LsrB research away from the previously well-characterized and accepted LsrB proteins to examine more distantly related LsrB-like proteins.[27] This was achieved by looking for orthologs to *Bacillus cereus* LsrB, a known AI-2 receptor protein of low sequence identity to *Salmonella enterica* ser. *Typhimurium* LsrB. Using this technique, the Miller/Xavier collaboration successfully identified the *Clostridium saccharobutylicum* LsrB protein which has since been proven to act as an LsrB protein (Inês Torcato, Unpublished Data).

More recent work done by Meghann Kasal from the Miller group in Swarthmore has aimed to examine *T. composti* LsrB.[41] The study of *T. composti* is ambitious, as it is the least conserved protein that still registered as a potential LsrB ortholog in the KEGG sequence analysis. The *T. composti* putative LsrB only has a 17% sequence identity with canonical *S. Typhimurium* LsrB, bringing into question its identity as a potential LsrB protein.[42,43] In addition to low sequence identity, *T. composti* only shares two of the six binding pocket interactions with canonical *S. Typhimurium* LsrB. This binding pocket variation could significantly alter the binding interactions observed between *T. composti* LsrB and AI-2. Demonstrating the function of *T. composti* LsrB in binding AI-2 would

help build the understanding of AI-2 quorum sensing and potentially offer another gateway into increasingly variant putative LsrB proteins.

Preliminary screening of potential LsrB candidates can be conducted using a bioassay that probes for AI-2 binding.[44] The assay functionalizes the bioluminescent response of *Vibrio harveyi* in the presence of AI-2 to quantify AI-2 bound to putative LsrB proteins. Potential LsrB orthologs can be denatured to release the AI-2 molecule which will then cause a bioluminescent response in the *V. harveyi*, demonstrating that AI-2 was bound. The standard method of denaturation is done with heat. Raising the temperature of a sample to 70ºC causes the protein to unfold, thereby releasing the bound AI-2 molecule and allowing uptake by the *V. harveyi*.[44] This method of denaturation is potentially flawed, however, when working with a protein from a thermophile, such as *T. composti*. *T. composti* naturally inhabits environments ranging from 32ºC to 60ºC,[45] therefore *T. composti* proteins must be stable even at these elevated temperatures.[46] The goal set forth in the present section is twofold. First, this section looks to validate an alternative technique to denature potential LsrB orthologs when heat denaturation does not suffice. Second, in this section the putative *T. composti* LsrB protein is probed for AI-2 binding as a preliminary result suggesting LsrB identity.

MATERIALS AND METHODS

Protease Trials

Proteases were screened for efficacy in cutting LsrB using SDS-PAGE. Samples of *Escherichia coli* LsrB were concentrated to 10mg/mL using a 10kD spin concentrators and then supplemented with protease. The proteases tested were proteinase K (Sigma), protease from *Bacillus licheniformis* (protease) (Sigma), and trypsin (Sigma). Proteases were added in 1:100 and 1:1000 molar ratios and allowed to cut at room temperature for

one hour. Time points were taken at 1, 5, 10, 30, and 60 minutes and samples were heated to inactivate proteases.

Sample Preparation

Samples were prepared from protein expressed and purified as described in Chapter 2 and Chapter 5. Trials were separated into several categories including protease, heat, protease and heat, flowthrough, and control. Positive control samples were prepared from *E. coli* LsrB expressed in cells producing AI-2 (LuxS+). Negative controls were prepared from *T. composti* LsrB expressed in cells without the ability to produce AI-2 (LuxS-). Experimental samples were prepared from *T. composti* expressed in LuxS+ *E. coli*. All samples were concentrated to 10mg/mL to control for any potential differences in observed signal. Protease treated samples received protease or proteinase K in a molar ratio of 1:100 and then allowed to cut at room temperature for 30 minutes. Heated samples were heating on a 70°C heat block for 10 minutes and centrifuged to remove denatured protein. Double experimental samples received protease first before denaturation at 70°C. The final experimental condition took the flowthrough from a sample spun until dry at 14,000 RPM in a 5kDa concentrator (Corning). Control conditions received the buffer that protein samples were prepared with (25mM Tris, 150mM sodium chloride, 1mM DTT, pH 8.0)

Assay Setup

Preparation for this assay began the night before each trial with starting an overnight sample of the *V. harveyi* to be assayed. Overnights were started from frozen stock of *V. harveyi* MM32 cells in 5mL of AB medium [1g casamino acids (BD), 6.15g magnesium sulfate heptahydrate (Sigma), 8.75g sodium chloride, 5mL of 100mM L-arginine (Sigma), 10mL of 50% glycerol (MP), 5mL 1M potassium phosphate (Sigma),

pH 7.5, per 500mL] in a 50mL Falcon tube. The culture was grown overnight at 30°C while shaking. The following day, the *V. harveyi* overnight was diluted 1:5000 and distributed as 90µL aliquots into a 96 well plate (VWR). Each well then received 10µL sample, bringing the final volume to 100µL per well. The plate was covered using a clear, adhesive cover (ThermoFisher) and the plate was placed in a 30°C incubator. Bioluminescence was monitored using a 1420 Victor 2 Multilabel Counter luminometer (Wallac) with points taken every hour for eight hours.

Statistical Analysis

Variance among the data was initially calculated through an ANVOA. In samples with an observed difference, data was tested for normality before moving on to pairwise comparisons. Pairwise comparisons were made using the Student's t-test with Bonferroni correction. All statistical analysis was performed in KaleidaGraph (Synergy Software).[47]

RESULTS

Protease Denaturation Trials

The protease denaturation trials showed that the protease and proteinase K enzymes fully digested LsrB proteins from *E. coli* and *T. composti*. Trypsin, on the other hand, only demonstrated a loss of 10kDa from the full-length protein. Protease and proteinase K, which showed more complete proteolysis, were advanced to bioluminescence trials (Figure 3.1).

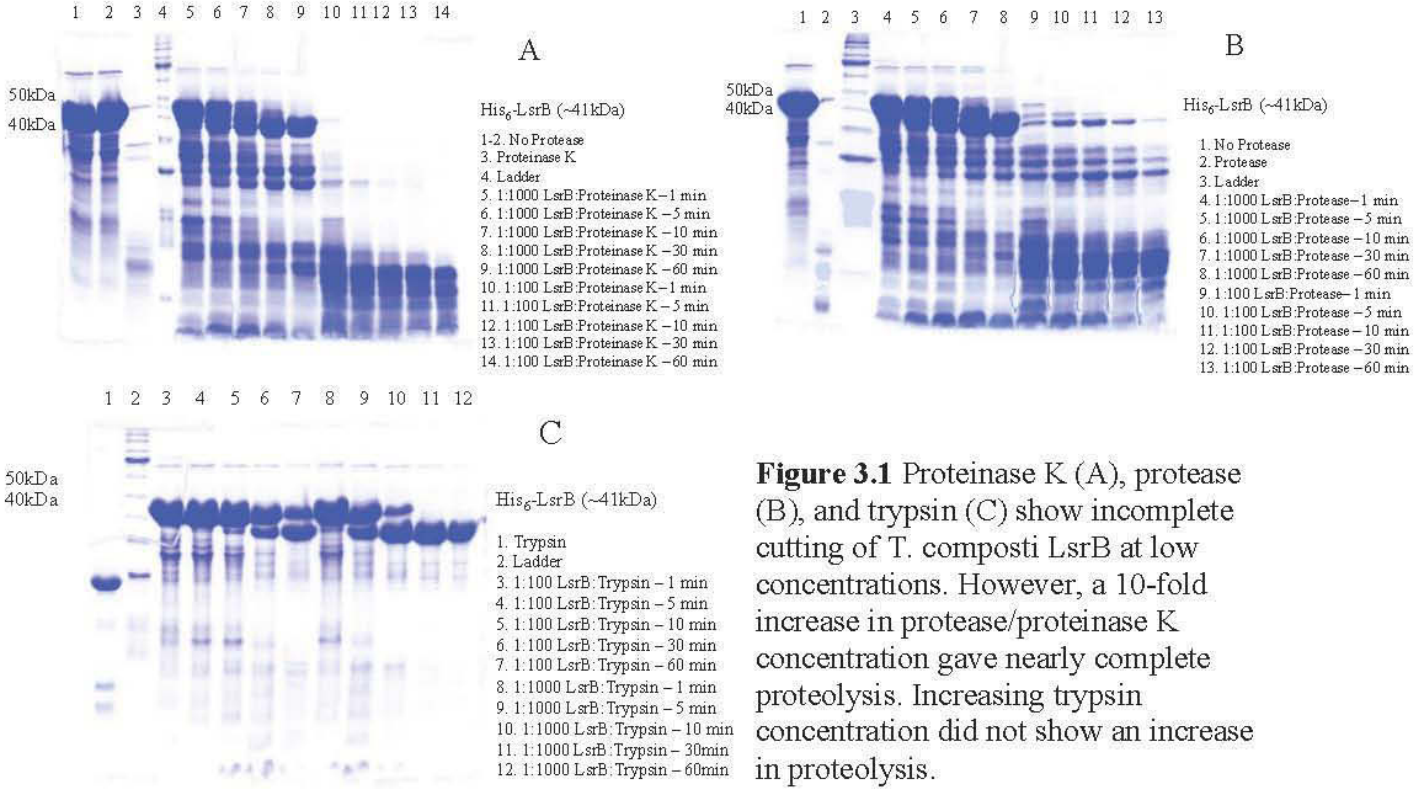

Figure 3.1 Proteinase K (A), protease (B), and trypsin (C) show incomplete cutting of T. composti LsrB at low concentrations. However, a 10-fold increase in protease/proteinase K concentration gave nearly complete proteolysis. Increasing trypsin concentration did not show an increase in proteolysis.

Analysis by ANOVA revealed differences between the experimental groups ($p<0.0001$, D.F.=71). The *V. harveyi* assay showed an increase in bioluminescence from LuxS- *T. composti* to LuxS+ *T. composti* LsrB samples for both protease ($p<0.0001$, D.F.=5, Table S3) and proteinase K ($p<0.0001$, D.F.=5, Table S3) treated samples. However, variability was also observed between *T. composti* growths under the same conditions, such as protease treated ($p<0.0001$, D.F.=5, Table S3) or proteinase K treated ($p<0.0001$, D.F.=5, Table S3). Examining the *E. coli* positive control, no significant difference was observed in response between protease and proteinase K treated samples ($p<0.0001$, D.F.=5, Table S3). Interestingly, response was observed in *E. coli* LsrB protein that was not treated with protease or heat relative to the LuxS- *T. composti* sample ($p<0.0001$, D.F.=5, Figure 3.2, Table S3). This result prompted further experimentation around this "no treatment" condition.

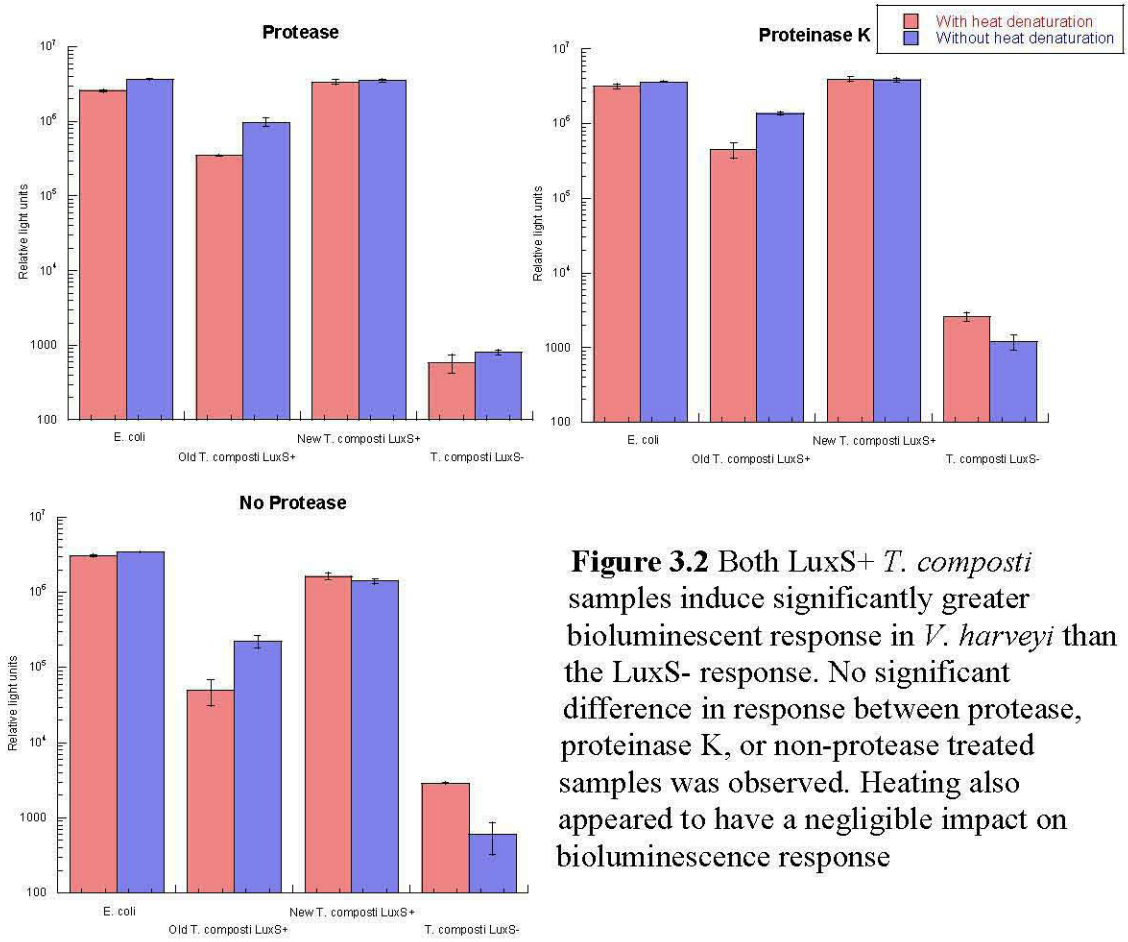

Figure 3.2 Both LuxS+ *T. composti* samples induce significantly greater bioluminescent response in *V. harveyi* than the LuxS- response. No significant difference in response between protease, proteinase K, or non-protease treated samples was observed. Heating also appeared to have a negligible impact on bioluminescence response

Trials Without Denaturation

Further experimentation focused on repeating observed results that non-denatured LsrB protein from *E. coli* and LuxS+ *T. composti* induced bioluminescence in *V. harveyi*. To probe this hypothesis further, this experiment further tested whether flow through from LuxS+ samples could elicit the bioluminescent response. The untreated *E. coli* ($p<0.0001$, D.F.=5, Table S4) and *B. anthracis* ($p<0.0001$, D.F.=5, Table S4) samples elicited a significantly greater bioluminescence response from the *V. harveyi*. Additionally, there was no observed difference between the no-treatment and flow through samples in *E. coli* ($p=1$, D.F.=5, Table S4) or *B. anthracis* ($p=1$, D.F.=5, Table S4) samples. The *T. composti* flow through ($p=0.2123$, D.F.=5, Table S4) and un-treated

samples (p=1, D.F.=5, Table S4) showed no significant difference from the blank sample. Though not statistically significant, there was a qualitatively observed increase in bioluminescence in the *T. composti* samples (Figure 3.3).

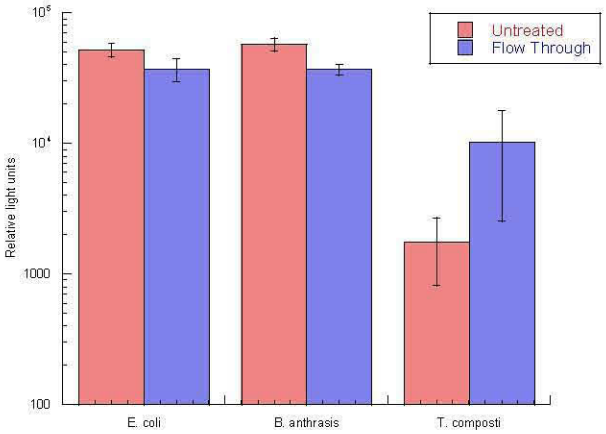

Figure 3.3 Untreated LsrB samples from *E. coli* and *B. anthracis* showed no significant difference between untreated protein and flowthrough samples, both of which showed significantly great bioluminescent response from the blanks. However, similar to the variability observed in Figure 3.2, the *T. composti* samples here vary significantly not only from each other, but also from the positive controls.

DISCUSSION

The bioluminescence assay demonstrated two primary results of interest. First, it demonstrated that LuxS+ *T. composti* LsrB does elicit a bioluminescent response from *V. harveyi*. This result suggests that *T. composti* is binding AI-2, a strong first indicator that its function as an AI-2 receptor molecule has been conserved despite the low sequence similarity to *S. Typhimurium* LsrB. However, unlike the *E. coli* LsrB samples, there was a discrepancy observed between from one protein growth to another. One possible explanation for this difference is the existence of another variant of the AI-2 signaling molecule, similar to the borated and non-borated forms of AI-2. This could help explain the difference in observed response, with another element determining AI-2 binding that is not yet appropriately controlled for in growing conditions.

The second interesting result presented here is the discovery that denaturation of potential AI-2 receptors is not necessary to allow the molecule to be released. This is a potential update to the procedure initially validated by the Bassler laboratory at Princeton

University, simplifying this assay by removing the denaturation step altogether. Preliminary results also appear to indicate that heat may degrade the AI-2 molecule, slightly, but not significantly, decreasing observed signal relative to the samples denatured by protease only. More trials need to be conducted to reinforce the benefits of foregoing heat-denaturation, but initial results suggest that avoiding denaturation entirely affords equal if not better results than the canonical heat denaturation.

Ch. 4 Analysizng *Thermobacillus composti* LsrB Phospho-AI-2 binding through Isothermal Titration Calorimetry Analysis

BACKGROUND

Following the positive result observed in the *Vibrio harveyi* bioluminescence assay, the next goal was to obtain a more quantitative value to characterize the binding interaction between AI-2 and *T. composti* LsrB. ITC was used to accomplish this task.[40]

ITC has been used previously to characterize the binding interaction between proposed LsrB proteins and AI-2. Prior to the arrival of the ITC at the Swarthmore Department of Chemistry and Biochemistry, the Miller group sent samples of LsrB orthologs to the Xavier laboratory in Portugal for ITC analysis. This technique has yielded values for several putative LsrB proteins, most recently demonstrating the binding between *Clostridium saccharobutylicum* LsrB and AI-2 (Inês Torcato, Unpublished Data). The present section aims to further demonstrate AI-2 binding by the putative *T. composti* LsrB protein, as well as obtain quantitative data, the dissociation constant (K_D), to further characterize the binding interaction.

MATERIALS AND METHODS

Preparation of the ITC Sample

LsrB protein samples were concentrated to 100μM in a 10kDa spin concentrator. All samples were equilibrated into the ITC buffer (25mM sodium phosphate, 150mM sodium chloride, 1mM β-mercaptoethanol, pH 8.0) using Slide-A-Lyzer dialysis cassettes (ThermoFisher). Samples were dialyzed in the ITC buffer in a 1:500 ratio for two two-hour periods before a final, overnight exchange period.[48]

Synthetic AI-2 was thawed and diluted to a final concentration of 800μM (ITQB).[49] Further trials used LuxS+ *T. composti* LsrB flowthrough to act as the ligand.

Samples were prepared by first cutting LuxS+ and LuxS- *T. composti* at a concentration of 200μM with a 1:100 molar ratio of proteinase K. After 30 minutes of cutting at room temperature, samples were spun until dry, about 15 minutes. Supernatant was then taken and acted in place of the ligand for the ITC experiments.

ITC Parameters

All ITC experiments were conducted with the MicroCal PEAQ-ITC (Malvern) at 4°C with a reference power of 10μcal/second. The cell was loaded with 300μL of LsrB receptor protein prepared as described previously.[50] 60μL of sample was loaded into the syringe, and the run was set up for 19 injections while mixing at 750 RPM. After an initial injection of 0.4μL, the remaining 18 injections were 2μL each. Analysis was conducted in the Microcal ITC software at the conclusion of each experiment.

RESULTS

The positive control sample of *C. saccharobutylicum* gave a sigmoidal titration curve, characteristic of a binding interaction. From this titration curve, ΔH was calculated to be -7.76±0.125kcal/mol and K_D was calculated to be 150±29.4nM. The same experiment conducted with LuxS- *T. composti* LsrB showed a less sharp titration curve and gave a calculated ΔH of -0.69±0.103kcal/mol (Figure 4.1). However, Microcal ITC analysis output a K_D of 4.45±3.02μM, corresponding to approximately 10-fold lower binding. However, both *C. saccharobutylicum* and *T. composti* had similar observed binding stoichiometry, with values of 0.820±0.0036 and 0.962±0.073 respectively.

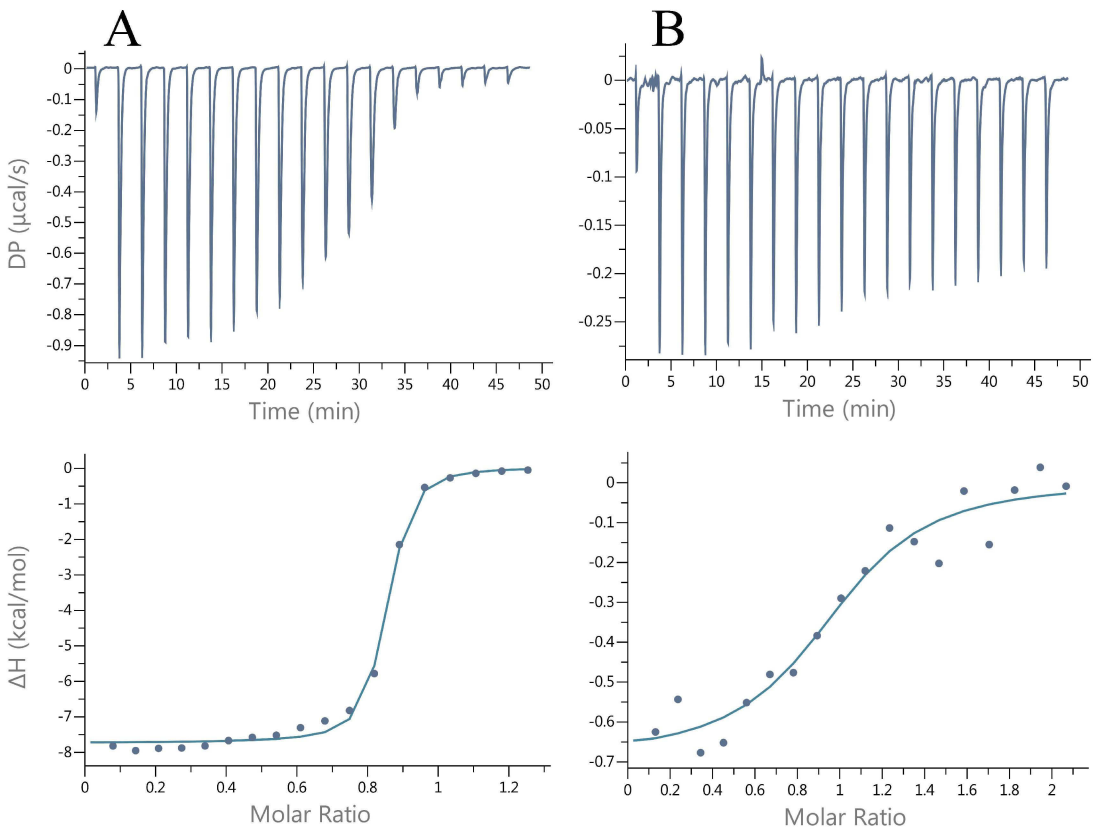

Figure 4.1 Both *C. saccharobutylicum* (A) and *T. composti* (B) show binding interactions as calculated by the Microcal ITC analysis software. However, the curve generated for *T. composti* and the released energy per injection are much weaker when compared to *C. saccharobutylicum*.

The flowthrough samples saw no obvious binding interactions. The graph of the energy released did not show the curve characteristic of binding as observed in the *C. saccharobutylicum* sample. Additionally, binding energies observed between the LuxS+ flowthrough and the LuxS- flowthrough were approximately equal, further suggesting a lack of observed binding (Figure 4.2).

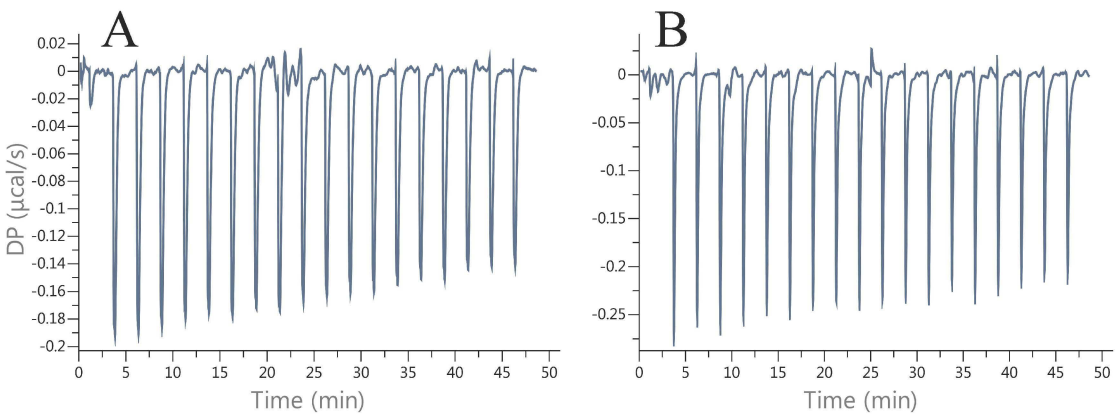

Figure 4.2 Protease treated LuxS- (A) and LuxS+ (B) *T. composti* flowthrough did not see the dramatic decrease in energy released per injection seen in the *C. saccharobutylicum* sample. The initial energy released per injection was roughly 4-fold lower in both of these samples than for *C. saccharobutylicum*

DISCUSSION

Although the Microcal ITC analysis software reported binding between AI-2 and *T. composti* LsrB, several factors challenge this conclusion. First, while a titration curve was generated from the AI-2 injection data into LuxS- *T. composti*, it did not take the sharp sigmoidal shape observed in the *C. saccharobutylicum* injection. Additionally, the ΔH of the *C. saccharobutylicum* binding interaction was 10-fold higher than that reported for *T. composti*. Finally, the initial energy released per injection does not appear to differ greatly between LuxS- flowthrough and AI-2 injections into LuxS- *T. composti* LsrB, while the energy released for *C. saccharobutylicum* is approximately 4-fold greater.

While these data seems to show that AI-2 is not binding, there are a few other factors to consider. While the curve generated by AI-2 addition to *T. composti* LsrB is not as sigmoidal as that of *C. saccharobutylicum*, it does register as weak binding with a dissociation constant of 4.45±3.02µM. What appears to be no binding could instead be weak binding.[51] This could potentially be due to *T. composti* LsrB recognizing a novel

form of AI-2. This would be similar to the difference between the borated and non-borated forms observed earlier.

The denatured flowthrough trials were designed to address the possibility of an AI-2 ortholog binding. While the protease digested flowthrough trials showed no binding, they relied on injecting an unknown concentration of an impure sample into the ITC cell. Thus, it is hard to know whether the lack of observed binding was due to a lack of affinity between AI-2 and *T. composti* LsrB, or simply a lack of ligand introduced to the ITC cell.[19]

The alternate AI-2 adduct theory is additionally promising as an explanation to another unexplained result observed in the previous chapter. Assuming that *T. composit* LsrB is binding an alternative form of AI-2, there would necessarily be some time spent converting it to the AI-2-borate needed to induce luminescence in *V. harveyi*, which could help explain the consistently lower intensity of bioluminescence. While interesting in theory, further experimentation was necessary to elucidate the binding interaction between *T. composti* LsrB and its ligand. To this end, further efforts focused on crystallography as a method to visualize this binding interaction.[52]

Ch. 5 Cloning and Expression of Truncated *Thermobacillus composti* LsrB

BACKGROUND

With a binding interaction theorized between the *T. composti* LsrB protein and an AI-2 analog, the next piece of the puzzle was to demonstrate binding, identify the ligand bound, and characterize the binding through structural characterization. Canonical *Salmonella enterica* ser. *Typhimurium* LsrB has been demonstrated to undergo a conformational change upon AI-2 binding, closing in around AI-2.[53] Demonstrating a similar conformational change from apo to holo, or potentially observing the AI-2 molecule bound to the putative *T. composti* LsrB protein, would act as definitive evidence binding. These data would also allow further quantitative experiments to hone in on the specific ligand binding.

Previous attempts at crystallization of *T. composti* LsrB by Meghann Kasal focused on a truncation that excluded the signaling molecule sequence encoded for by the *lsrB* gene.[41] These crystallization attempts were unsuccessful. The work presented in this section aimed to generate truncations of the *T. composti* LsrB protein to facilitate crystallization. The theory supporting this is the same leading to the generation of the truncations of LsrE in chapter 2. Removing intrinsically disordered regions may facilitate packing and, therefore, more readily allow crystal formation. This also provided an opportunity to validate another cloning technique for the Miller Laboratory in using ligation independent cloning (LIC) rather than gateway cloning pathway discussed in Chapter 2.[54]

MATERIALS AND METHODS

Creation of Truncated T. composti LsrB Truncation

T. composti LsrB crystallizability was predicted for potential truncations using XtalPred-RF. This server compared previously crystallized proteins and generated a crytallizability factor for each truncation. From this analysis, one N-terminal truncation was predicted to show higher crystallizability (Figure 5.1). [33,55]

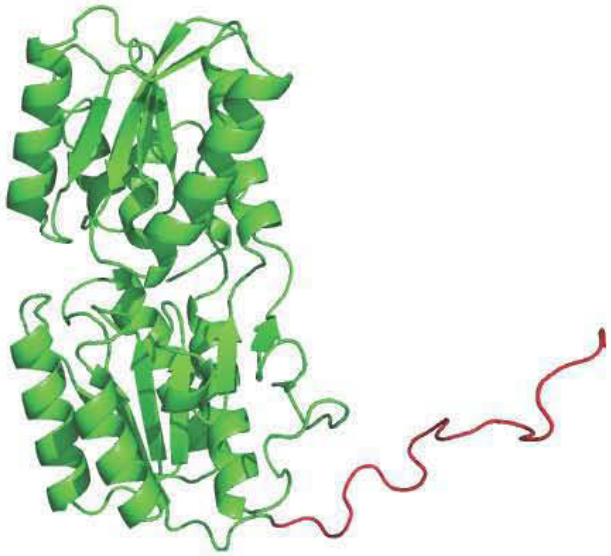

Figure 5.1 The structure of *T. composti* LsrB as predicted by Phyre[2]. The red region indicates the truncation created to facilitate crystallization.

Primers were ordered from Sigma Aldrich to generate truncated *T. composti* LsrB with restriction sites for LIC. These new primers were used to amplify the truncated *T. composti* LsrB construct from genomic DNA by PCR (Table S1). The Fera laboratory from Swarthmore College provided pLIC-Tr3a-HA vector. Vector was digested with the SspI-HF restriction enzyme (NEB) to produce a linear plasmid with blunt ends. Both vector and amplified insert were run on 0.8% low melt TAE agarose gels (Sigma). Desired components were isolated using the QIAquick Gel Extraction Kit (Qiagen). Both the vector and insert were then incubated with T4 DNA polymerase (NEB) to create the complementary regions. Vector and insert were then mixed to facilitate insertion into the vector.

With the insert fused into the vector, plasmid was transformed into DH5α *E. coli* cells and plated on agar plates to grow overnight at 37ºC. Colonies were selected from the plate and 5mL cultures were inoculated with individual colonies and grown overnight at 37ºC. Cultures were centrifuged at 4000 RPM and plasmid DNA was purified using the QIAprep Spin Miniprep Kit. Purified plasmid was sequenced, and then purified plasmids were transformed into Ca^{2+} competent BL21 (DE3) *E. coli* cells for protein expression.

Growth and Expression of Truncated T. composti LsrB

Protein expression began by inoculating 100mL of LB supplemented with 100µL of 100mg/mL ampicillin with the BL21 DE3 *E. coli* cells coding for truncated *T. composti* LsrB. After shaking at 37ºC overnight, 1L cultures supplemented with 1mL of 100mg/mL ampicillin were inoculated with 10mL of the over-night growth. Cultures grew at 37ºC while shaking for two hours until the optical density (OD_{595}) reached 0.5, at which point the temperature was dropped to 30ºC. Cultures grew for another hour until OD_{595} reached 1.0, at which point each 1L flask was inoculated with 100µL of IPTG. The induced cultures grew at 30ºC for eight hours before final harvesting by centrifugation at 4,000 RPM for 10 minutes. Pellets were resuspended in significantly reduced LB media and centrifuged again at 4,000 RPM for 30 minutes in a 50mL Falcon tube. Supernatant was decanted, and final pellets were stored at -80ºC for future purification.

Purification of Truncated T. composti LsrB

Cells were resuspended in 20mL of lysis buffer (50mM sodium phosphate, 300mM sodium chloride, 10mM imidazole, 1.4mM β-mercaptoethanol, pH 8.0) via vortexing. Once resuspended, cells were supplemented with 10µg/mL DNAse and

10μg/mL leupeptin prior to lysing. Resuspended cells were then lysed using the M-110Y microfluidizer before centrifugation for 30 minutes at 18,000 RPM.

Following centrifugation, supernatant was decanted from the cellular debris and run over three Ni-NTA agarose columns that had been pre-equilibrated in lysis buffer in series. Following supernatant, weakly binding impurities were eluted using three 5mL aliquots of wash buffer (50mM sodium phosphate, 300mM sodium chloride, 20mM imidazole, 1.4mM β-mercaptoethanol, pH 8.0) per column. Protein was then eluted from the column with four 2mL aliquots of elution buffer (50mM sodium phosphate, 300mM sodium chloride, 250mM imidazole, 1.4mM β-mercaptoethanol, pH 8.0). Protein yields were determined by UV-vis spectroscopy and purity was assessed by SDS-PAGE.

Fractions containing protein were pooled, and were transferred into buffer-swap buffer (25mM Tris, 150mM sodium chloride, 1mM DTT, pH 8.0) using the HiPrep 26/10 size exclusion column (SEC). Protein content was again assessed using SDS-PAGE and UV-vis, relevant fractions were pooled, and tobacco etch virus (TEV) protease was added in a 1:100 molar ratio to remove the His_6 tag. Cutting was visualized using SDS-PAGE and cut protein was again purified by Ni-NTA agarose columns. Unlike previously, with the tag removed the *T. composti* LsrB was expected to not bind to the Ni-NTA columns, instead appearing in the flowthrough. Protein was again assessed by SDS-PAGE and UV-vis spectroscopy and pooled accordingly.

Further purification was performed using ion exchange chromatography (IEC). Because this was a novel form of the protein, initial IEC runs were performed on the MonoQ anion exchange column (GE Life Science) before scaling up to the Source15Q. Initial conditions to carry out IEC were taken from prior purifications of the full-length construct carried out by Meghann Kasal. A gradient from 150mM to 1M sodium chloride

in Buffer A (25mM Tris, 1mM DTT, pH 8.0) was used for separation. Following IEC, final purification was done using SEC. Protein was concentrated to under 5mL and run over a Superdex 75 16/60. This final purification step also acted as a buffer exchange step into crystallization buffer (25mM Tris, 150mM sodium chloride, 1mM DTT, pH 8.0). Protein was concentrated to its final concentration of 20mg/mL using spin concentrators. Concentration was increased by centrifugation at 4000 RPM in 10 minute intervals. Final protein concentration was calculated using parameters calculated by ExPASy ProtParam (Table S2).

RESULTS

Optimization of Truncated T. composti LsrB Purification

The putative LsrB typically exhibited high solubility and, therefore, lent themselves readily to overexpression in *E. coli* models. This *T. composti* LsrB truncation continued this trend as it readily expressed soluble protein at temperatures higher than the LsrE growth described in Chapter 2, with yields obtained from 6L of growth in the range of 200 to 300mg of protein.

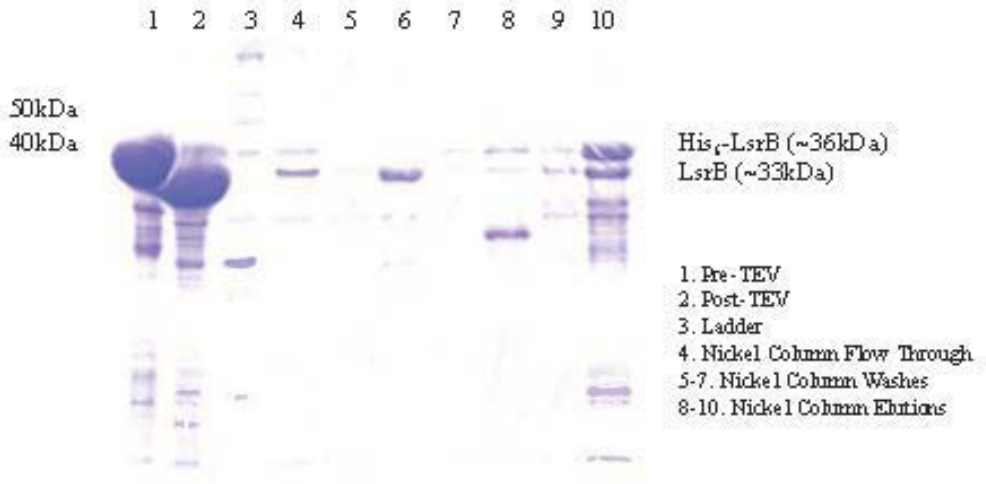

Figure 5.2 TEV protease cut *T. composti* LsrB with high efficiency even at low concentrations. Further purification by nickel columns showed good separation of LsrB from the His tag, TEV protease, and uncut His_6-LsrB.

The truncation of *T. composti* LsrB did not impair the removal of the His_6 tag, with TEV protease cleaving nearly all of the protein even at very low concentrations. In another defining feature setting this LsrB truncation apart from earlier work with LsrE, the second round of Ni-NTA columns resulted in excellent separation, with both the uncut LsrB protein as well as the TEV protease sticking to the column while the truncated *T. composti* LsrB came off in the flowthrough or with the first wash (Figure 5.2).

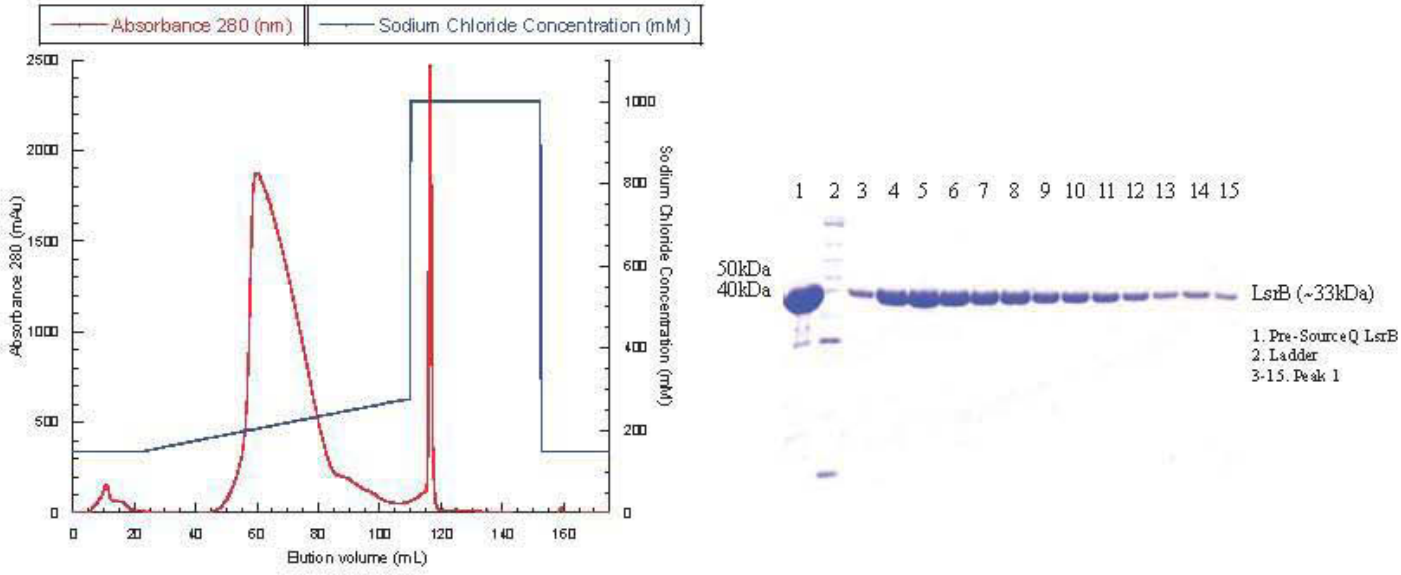

Figure 5.3 Anion exchange using the Source15Q showed high purification of LsrB from lower molecular weight contaminants. However, the peak identified as LsrB has an unidentified tailing region that does not show as a contaminant on SDS-PAGE gels.

Following initial purification of the TEV protease digested protein, anion exchange chromatography showed that the truncated *T. composti* LsrB eluted at approximately 300mM sodium chloride. Source15Q runs were then optimized to run a gradient from 150mM to 400mM sodium chloride, successfully removing several minor impurities. Purification at pH 8.0 yielded a large tailing region to the isolated protein peak, but SDS-PAGE analysis did not show any impurities accounting for this uneven peak (Figure

5.3).[56] Fractions following the peak were pooled separately and not used in subsequent crystallization attempts. Size exclusion chromatography attempted with the Superdex 75 column did not show any noticeable purification, and was subsequently removed from the purification procedure in favor of a simple buffer swap on the HiPrep 26/10 desalting column (Figure 5.4).

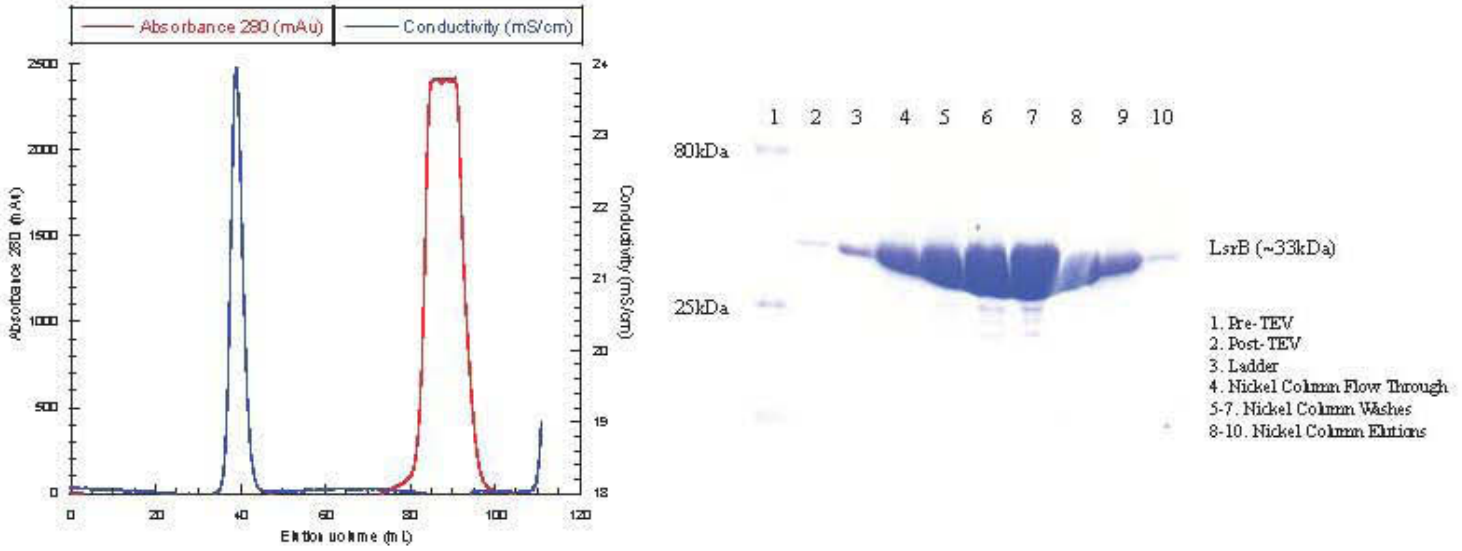

Figure 5.4 Purification by S75 16/60 SEC did not increase protein purity. The following analysis of the elution peak revealed a few lower molecular weight contaminants in low concentration. These were most likely not visualized following Source15Q due to the lower concentration.

DISCUSSION

This chapter reports the successful cloning, expression, and purification of truncated *T. composti* LsrB. The alternative cloning technique worked well, opening an alternative cloning pathway for future experimentation in the Miller laboratory. The purification procedure did not vary significantly from the purification procedure verified for the full length LsrB protein validated from Meghann Kasal. TEV protease digestion worked with high efficiency even at low concentrations, and Ni-NTA columns separated the non-tagged LsrB from the cleaved tag, the uncut protein, and the TEV protease.

One notable difference was the presence of the trailing region during the IEC separation. In the purification of full-length *T. composti* LsrB, separation of a major contaminant was observed at pH 8.0 by Source15Q anion exchange. However, in the truncation generated here, a peak with a large tailing region was observed instead of a symmetrical peak. This could be caused by low concentrations of contaminants, or possibly an overloading of the IEC. Further IEC optimization could be conducted through trials using different pH buffers, but pooling the tail region separately here afforded pure protein so further IEC optimization was unnecessary.

With the Superdex 75 purification not demonstrating any significant separation, further purifications simplified that step to a buffer exchange using the HiPrep 26/10 desalting column. This reduced the time required for purification while giving a final product of equal purity. Unlike the LsrE truncation discussed in Chapter 2, truncated *T. composti* LsrB showed high solubility even at concentrations approaching 100mg/mL. This, again, matched closely with the full-length construct. With the truncated *T. composti* LsrB purified and concentrated, attention could next turn towards crystallization.

Ch. 6 Crystallization and Diffraction of Truncated *Thermobacillus composti* LsrB

BACKGROUND

With the truncated *T. composti* LsrB expressed and purified, next steps turned towards crystallization and structure determination through x-ray diffraction. Initial crystallization attempts of full-length *T. composti* LsrB done by Meghann Kasal worked with protein concentrated to approximately 100mg/mL.[41] Even at these high concentrations, no promising pre-crystal conditions were observed. Because no promising conditions were observed in the full-length construct, work on the truncated construct began anew.

MATERIALS AND METHODS

Crystallization of Truncated T. composti LsrB

The Pre-Crystallization Test (Hampton) was used to find an approximate concentration of protein suitable for further screening. All initial crystal screens were performed using the Mosquito HTS crystallization robot (TTP LabTech) to set 200+200nL drops above 100µL reservoirs. Initial screening was performed with LuxS+ *T. composti* LsrB at a concentration of 20mg/mL. Preliminary screens were performed using the Crystal Index, the Crystal Screen 1 and 2, and the PEGRx Screen 1 and 2 (Hampton). Wells were allowed to equilibrate and results recorded periodically. Conditions that produced crystal precursors moved on to further screening and optimization. Finer optimization was also scaled up to 24-well trays with 2+2µL drops above 1mL wells. Varying salt and precipitant concentration around initial hits further refined the conditions to the optimal crystallization conditions. Final optimization was done by varying buffer pH around the targeted condition. Once suitable crystals formed,

they were collected manually in loops purchased from Hampton ranging in size between 0.2mm and 0.5mm. Crystals were either frozen directly from mother liquor or treated with glycerol supplemented mother liquor or paratone (Hampton) for additional cryoprotection. Crystals were then shipped in the CX100 dry shipper (MD). Diffraction data were collected at the Stanford Synchrotron Radiation Lightsource (SSRL) and Advanced Photon Source (APS) synchrotrons.

Crystal Diffraction and Initial Processing

Each crystal was briefly imaged at ϕ values of 0° and 90° to determine crystal quality. Crystals that produced diffraction patterns to a resolution of 3Å or better with single spots on the initial snapshots moved on for full data set collection. Starting angle and degree of oscillation were determined based on preliminary crystal metrics calculated by SSRL and APS. SSRL and APS gave initial diffraction statistics from the X-ray Detector Software. Collected data were transferred to Swarthmore servers for further processing. Molecular replacement was attempted using the Python-based Hierarchical Environment for Integrated Xtallography (Phenix) Phaser.[57]

RESULTS

Crystallization Screens and Optimization

Initial screens carried out with the Mosquito crystallization robot afforded several conditions of interest (Table S5). Further optimization was carried out on two conditions: 100mM BIS TRIS (VWR) pH 7.5, 200mM sodium chloride, 41% polyethylene glycol (PEG) 3350 (Aldrich); and 100mM 4-(2-hydroxyethyl)-1-piperazineethanesulfonic acid (HEPES) (JT Baker) pH 7.5, 200mM calcium chloride dehydrate (Fluka), 33% PEG 400 (Sigma). PEG concentrations were varied within a 3% range from the initial condition, while salt concentrations varied within a 100mM range. Once conditions that consistently

yielded promising crystals were determined, two alternative pH trials were attempted: increasing the pH to 8.5 and decreasing the pH to 6.5.

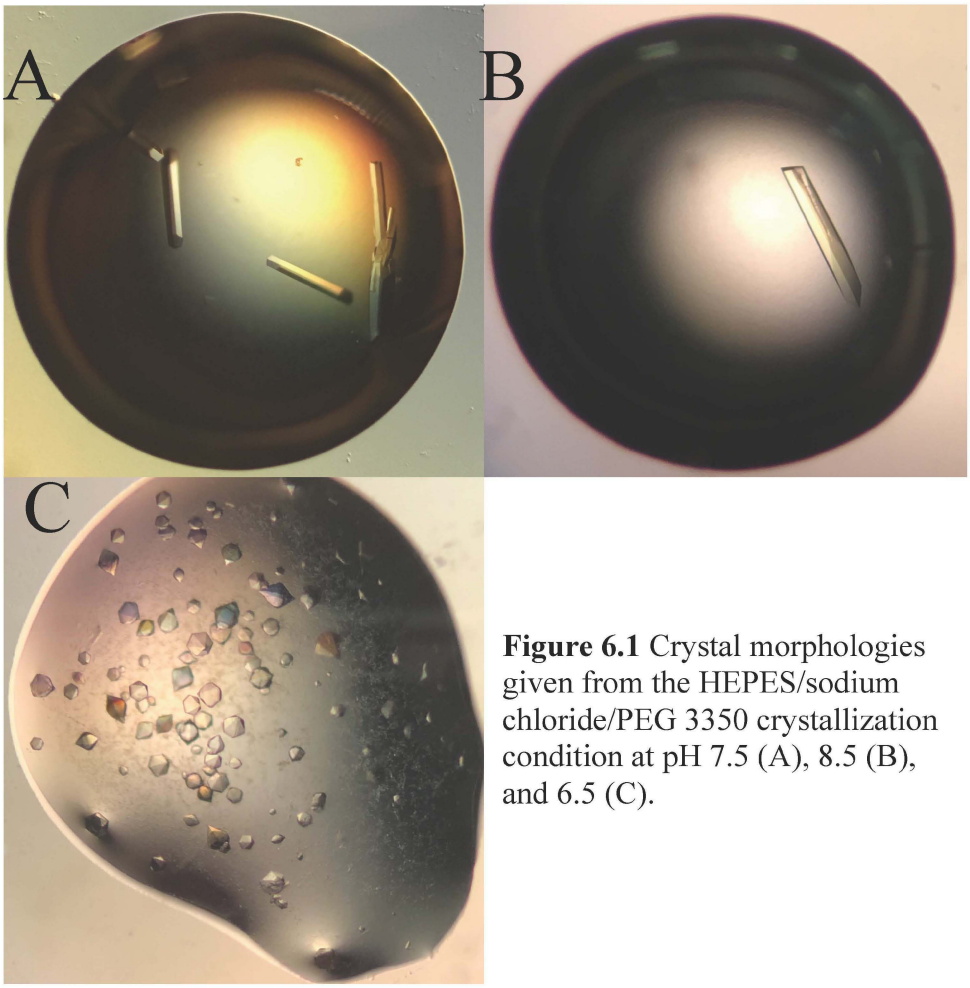

Figure 6.1 Crystal morphologies given from the HEPES/sodium chloride/PEG 3350 crystallization condition at pH 7.5 (A), 8.5 (B), and 6.5 (C).

Both pH 6.5 and pH 8.5 yielded crystals in the first condition, with all conditions giving crystals of different morphologies (Figure 6.1). No crystals formed in the second condition when the pH was reduced to 6.5. The second condition gave crystals of similar morphology when the pH was increased to 8.5 (Figure 6.2).

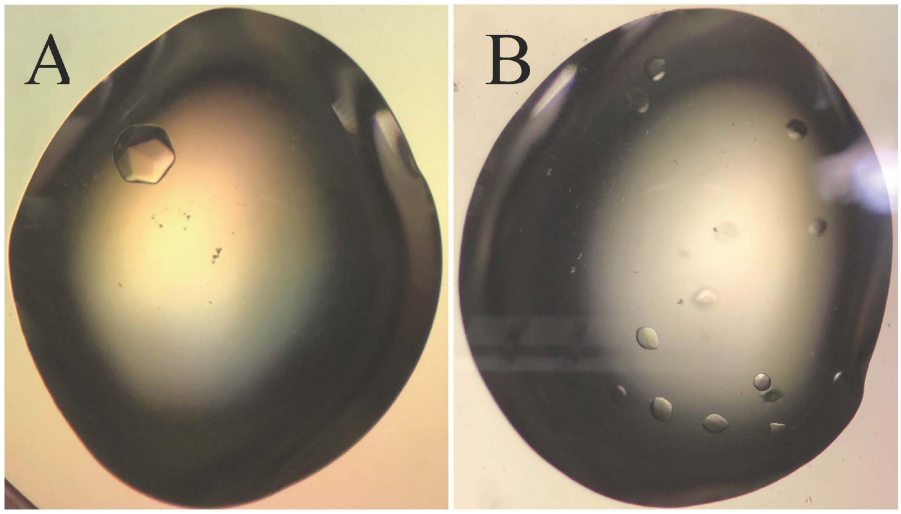

Figure 6.2 Crystal morphologies observed from the HEPES/calcium chloride monobasic/PEG 400 condition for both pH 7.5 and 8.5. Some of these crystals appeared symmetrical with no apparent abnormalities (A), but others showed signs of satellite or capping crystals (B).

Crystal Diffraction and Initial Processing

Crystals grown in the BIS TRIS, sodium chloride, PEG 3350 condition were analyzed at SSRL 9-2. No crystals from this first collection showed diffraction patterns past 3.0Å. Many crystals from this collection were damaged from ice formation, and those crystals that were not damaged afforded generally weak diffraction patterns.

Table 6.1 Diffraction statistics from a average resolution representative crystal

Parameter	Overall	Inner Shell	Outter Shell
High Resolution Limit (Å)	2.56	8.87	2.56
Low Resolution Limit (Å)	169.57	169.57	2.68
Completeness (%)	99.1	99.9	92.9
Multiplicity	11.9	10.7	4.4
I/σ	15.5	34.7	1.8
R_{merge}	0.106	0.057	0.432

Crystals grown in the HEPES, sodium chloride dehydrate, PEG 400 had diffraction data collected at APS on beam-line 24-ID-C. These crystals gave significantly stronger diffraction patterns than those analyzed at SSRL. The best crystals from this new crystallization condition showed diffraction spots out to 1.88Å. However, while single

diffraction spots were observed in some orientations, most crystals showed clusters of spots in some orientations (Figure 6.3). While this peculiar diffraction pattern was observed in many of the collected crystals, a few gave data suitable for molecular replacement attempts. Table 6.1 gives the diffraction statistics for a representative lower resolution crystal.

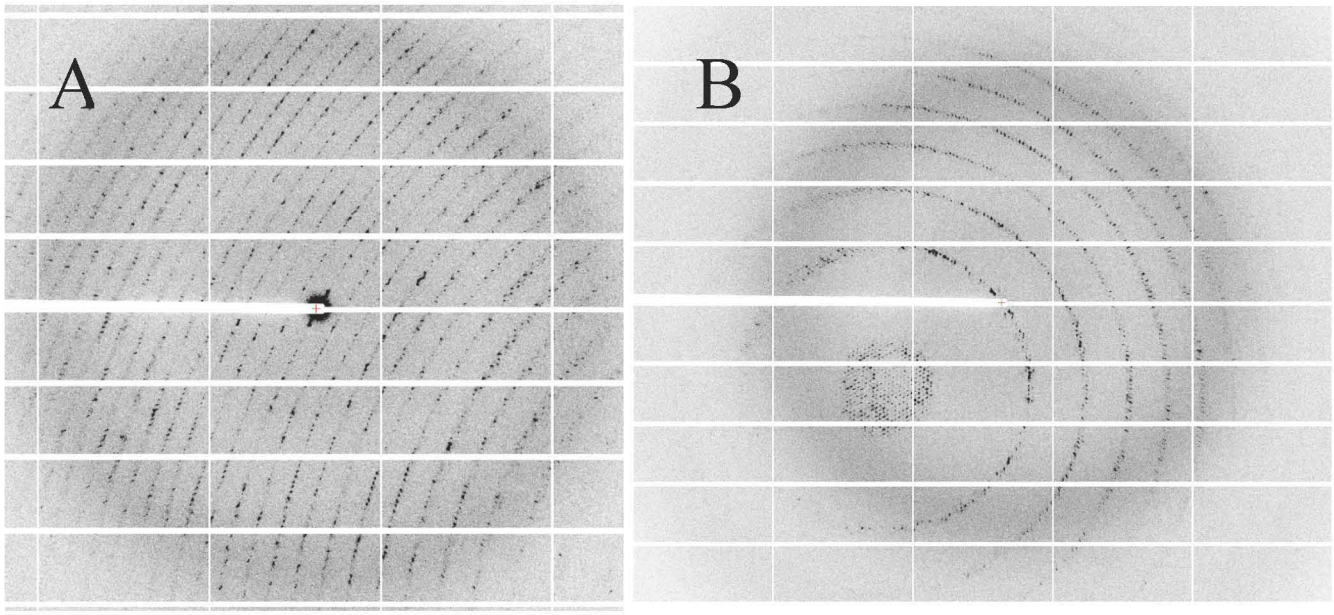

Figure 6.3 Data collected from many crystals formed in the HEPES/calcium chloride monobasic/PEG 400 condition showed single diffraction spots in in some orientations (A) and groups of spots in others (B).

DISCUSSION

This chapter demonstrated the utility of terminal truncation in the formation of crystals. Removing a putatively disordered region of the *T. composti* LsrB protein allowed crystallization where previous attempts with the full-length construct had failed. Not only did this particular construct give crystals under one condition, it showed a marked increase in crystallizability with several conditions yielding crystal precursors and crystals suitable for diffraction coming from two distinct conditions (Table S5).

However, while crystallization of this LsrB construct progressed with relative ease, difficulties arose during diffraction. The crystals afforded by the first condition and visualized at SSRL gave no usable data. These crystals showed a significant amount of ice formation, despite a high concentration of PEG 3350. However, even crystals that had been cryoprotected gave poor diffraction patterns and ultimately yielded no useful data. Further work on this initial crystallization condition should explore alternative cryoprotection options to attempt to obtain a clean diffraction pattern without the significant ice formation.

The crystals afforded by the second crystallization condition and analyzed at APS tell a different story. Ice formation was not an issue, most likely attributable to the use of the lower molecular weight PEG 400. Not only was ice formation a non-issue, but diffraction patterns collected were strong. The best data set collected showed diffraction to 1.88Å. While these data show a marked improvement over the crystals sent to SSRL, the data from APS were not flawless. The crystals examined all showed a peculiar diffraction pattern that appeared to arise periodically throughout the x-ray's oscillation. Two factors could have caused this observed diffraction pattern. The first possibility is that this crystal formed as two unaligned lattices, causing splitting of Bragg diffraction angles. Another possibility is that the diffracted crystals formed with satellite crystals. Again, the formation of multiple lattices causes multiple spots where only one should be observed.[58]

Initial molecular replacement attempts were conducted in the Phenix Phaser software using the parameters calculated by APS. These attempts did not yield any matches. While the current data do not allow for structural determination, there are two avenues that could potentially take the present understanding of the situation to allow

future structural determination. The primary focus of future work is to collect from more crystals in the hopes that the observed aberrant diffraction pattern is not present in all cases.

Should future data collection attempts of the current crystals continue to prove fruitless, revisiting the crystallization conditions would be the next avenue to pursue. A first attempt using the truncated *T. composti* LsrB construct grown with media containing selenomethionine would facilitate molecular replacement through single or multiple anomalous dispersion.[59] Other crystallization conditions could be elucidated through additive screens, which were not explored in the crystallization attempts of truncated *T. composti* LsrB. Building upon the several conditions that afforded crystals or crystal precursors, an additive screen could assist in better crystal formation. Lastly, aiding in crystal formation through crystal seeding presents another potential optimization step that was not explored in this chapter.[60]

It is important to note that while the structure was not determinable from this data, the crystallization and data collection of truncated *T. composti* LsrB crystals marks a notable improvement from the work previously done with the full-length construct. Future work to crystallize, diffract, and solve the structure of this construct poses additional incentive, as that solution could then potentially aid in de-convoluting the 1.88Å diffraction pattern collected here. With a structure at this resolution, the presence of any bound ligand, and potentially the ligand identity, would be determinable. This could demonstrate AI-2 binding to *T. composti* LsrB and provide insight into the observed discrepancy between the results from the *Vibrio harveyi* bioluminescence assay and ITC.

Ch. 7. Conclusions and Future Directions

This work done with the LsrE and LsrB proteins from *Salmonella enterica* ser. *Typhimurium* and *Thermobacillus composti* respectively has contributed to our understanding of each of these proteins, particularly in relation to their ability to readily overexpress in *E. coli* expression models and their ability to readily form crystals. However, this work has also demonstrated many potential pitfalls of protein research, with LsrE truncations showing reduced solubility when overexpressed and LsrB affording crystals, but proving difficult to convert diffraction patterns into solved electron density maps.

The *S. Typhimurium* LsrE project saw difficulties in the expression of soluble protein. Even in the constructs where soluble protein was obtained, removal of the His-MBP tag caused protein to precipitate even at very low concentrations. While attempts at LsrE truncation proved fruitless, future work should direct attention towards functionality assays instead. Specifically, examining any binding interactions between AI-2 and AI-2 derivatives with LsrE through kinetics studies would provide evidence that LsrE plays a functional role in the AI-2 quorum sensing pathway and is not simply a vestigial protein.

While work with *S. Typhimurium* LsrE showed difficulties early on, work with *T. composti* LsrB showed promising results early on as the *Vibrio harveyi* bioluminescence assay suggested the presence of AI-2 bound. Further studies by ITC to demonstrate the binding interaction between *T. composti* LsrB with AI-2 did not show the clear binding interaction observed in other LsrB proteins. The truncated *T. composti* LsrB generated using ligation independent cloning worked well, not demonstrating the same solubility issues observed in the *S. Typhimurium* LsrE constructs. This truncated LsrB protein was

then crystallized under several conditions and diffraction patterns were collected. Difficulties arose in the interpretation of the diffraction data, as the highest resolution data showed highly split patterns, most likely due to multiple satellite crystals forming. These flaws likely caused trouble in solving the structure of the *T. composti* LsrB protein by molecular replacement. Moving forward with the *T. composti* LsrB project, future work should aim to take the preliminary crystals used for diffraction here and look to optimize them. This could take the form of simply collecting and image more crystals in an attempt to collect a data set that does not exhibit the peculiar diffraction pattern. Other future work could revisit the crystallization conditions and attempt to add in more factors through an additive screen to see if more structured single crystals would form. Either way, structural determination is within reach for *T. composti* LsrB given more time to optimize and visualize more crystals.

Despite difficulties encountered in both the *T. composti* LsrB project and the *S. Typhimurium* LsrE project, work on both proteins has expanded the understanding of how these proteins behave. With the discovery of more bacteria that use AI-2 quorum sensing to interact with their environment, increased understanding of the bacteria that use this pathway and better understanding of the proteins in this pathway will provide insight into how this pathway can be functionalized. Especially with the elucidation of the role that AI-2 quorum sensing plays in biofilm formation and bacterial virulence, furthering the understanding of proteins in this pathway will hopefully aid in the ability to better control these processes.

Acknowledgments

I would like to thank Professor Stephen Miller for taking me on and mentoring me for the past two years in lab. I would also like to thank Emily Gale and Meghann Kasal for providing experience as I first entered lab as a sophomore. Thanks to Kenji Yoshi, Steven Chen, and Eli Kissman, who acted as compatriots and friends in and out of lab. I would also like to thank Audrey Allen and Sam Tanner for their pioneering work with LsrE. Thanks to Professor Liliya Yatsunyk of Swarthmore College and Professor Matthew Neiditch of the New Jersey Medical School: Rutgers, who allowed me to collect diffraction data on their scheduled trips to APS and SSRL respectively. I want to extend a warm thanks to the combination of the Howard Hughes Medical Institute, the National Institute of Health, the Meinkoth Premedical Fund, and Swarthmore College for helping to fund my research while at Swarthmore. Thanks to Dr. Stephen Harrison for taking the time to read and discuss my thesis with me as a part of the Honors Program. Thank you to the Swarthmore College Department of Chemistry and Biochemistry class of 2018 for providing companionship through the ups and downs of Swarthmore. Finally, and most importantly, I would like to thank my family: Jill Petty, Chris Clayhold, and Zach Clayhold, for their love and support during my time at Swarthmore and in all of my endeavors. Without all of these individuals, I would have had no chance to be as successful as I have in my time at Swarthmore.

Literature Cited

(1) Nealson, K. H.; Platt, T.; Hastings, J. W. Cellular Control of the Synthesis and Activity of the Bacterial Luminescent System1. *J. Bacteriol.* **1970**, *104* (1), 313–322.

(2) Bassler, B. L.; Greenberg, E. P.; Stevens, A. M. Cross-Species Induction of Luminescence in the Quorum-Sensing Bacterium Vibrio Harveyi. *J. Bacteriol.* **1997**, *179* (12), 4043–4045.

(3) Ruby, E. G.; McFall-Ngai, M. J. A Squid That Glows in the Night: Development of an Animal-Bacterial Mutualism. *J. Bacteriol.* **1992**, *174* (15), 4865–4870.

(4) Engebrecht, J.; Nealson, K.; Silverman, M. Bacterial Bioluminescence: Isolation and Genetic Analysis of Functions from Vibrio Fischeri. *Cell* **1983**, *32* (3), 773–781.

(5) Miller, M. B.; Bassler, and B. L. Quorum Sensing in Bacteria. *Annu. Rev. Microbiol.* **2001**, *55* (1), 165–199.

(6) Fuqua, W. C.; Winans, S. C.; Greenberg, E. P. Quorum Sensing in Bacteria: The LuxR-LuxI Family of Cell Density-Responsive Transcriptional Regulators. *J. Bacteriol.* **1994**, *176* (2), 269–275.

(7) Nealson, K. H.; Hastings, J. W. Bacterial Bioluminescence: Its Control and Ecological Significance. *Microbiol. Rev.* **1979**, *43* (4), 496–518.

(8) Bassler, B. L.; Wright, M.; Showalter, R. E.; Silverman, M. R. Intercellular Signalling in Vibrio Harveyi: Sequence and Function of Genes Regulating Expression of Luminescence. *Mol. Microbiol.* **1993**, *9* (4), 773–786.

(9) Surette, M. G.; Miller, M. B.; Bassler, B. L. Quorum Sensing in Escherichia Coli, Salmonella Typhimurium, and Vibrio Harveyi: A New Family of Genes Responsible for Autoinducer Production. *Proc. Natl. Acad. Sci. U. S. A.* **1999**, *96* (4), 1639–1644.

(10) Pereira, C. S.; Thompson, J. A.; Xavier, K. B. AI-2-Mediated Signalling in Bacteria. *FEMS Microbiol. Rev.* **2013**, *37* (2), 156–181.

(11) J W Costerton; Z Lewandowski; D E Caldwell; D R Korber; Lappin-Scott, and H. M. Microbial Biofilms. *Annu. Rev. Microbiol.* **1995**, *49* (1), 711–745.

(12) Prouty, A. M.; Schwesinger, W. H.; Gunn, J. S. Biofilm Formation and Interaction with the Surfaces of Gallstones by Salmonella Spp. *Infect. Immun.* **2002**, *70* (5), 2640–2649.

(13) Zhu, J.; Miller, M. B.; Vance, R. E.; Dziejman, M.; Bassler, B. L.; Mekalanos, J. J. Quorum-Sensing Regulators Control Virulence Gene Expression in Vibrio Cholerae. *Proc. Natl. Acad. Sci. U. S. A.* **2002**, *99* (5), 3129–3134.

(14) Wang, X.; Li, X.; Ling, J. Streptococcus Gordonii LuxS/Autoinducer-2 Quorum-sensing System Modulates the Dual-species Biofilm Formation with Streptococcus Mutans. *J. Basic Microbiol.* **2017**, *57* (7), 605–616.

(15) Fitts, E. C.; Andersson, J. A.; Kirtley, M. L.; Sha, J.; Erova, T. E.; Chauhan, S.; Motin, V. L.; Chopra, A. K. New Insights into Autoinducer-2 Signaling as a Virulence Regulator in a Mouse Model of Pneumonic Plague. *mSphere* **2016**, *1* (6), e00342-16.

(16) Ma, R.; Qiu, S.; Jiang, Q.; Sun, H.; Xue, T.; Cai, G.; Sun, B. AI-2 Quorum Sensing Negatively Regulates Rbf Expression and Biofilm Formation in Staphylococcus Aureus. *Int. J. Med. Microbiol.* **2017**, *307* (4–5), 257–267.
(17) Wu, X.; Lv, X.; Lu, J.; Yu, S.; Jin, Y.; Hu, J.; Zuo, J.; Mi, R.; Huang, Y.; Qi, K.; et al. The Role of the PtsI Gene on AI-2 Internalization and Pathogenesis of Avian Pathogenic Escherichia Coli. *Microb. Pathog.* **2017**, *113*, 321–329.
(18) Meng, L.; Du, Y.; Liu, P.; Li, X.; Liu, Y. Involvement of LuxS in Aeromonas Salmonicida Metabolism, Virulence and Infection in Atlantic Salmon (Salmo Salar L). *Fish Shellfish Immunol.* **2017**, *64*, 260–269.
(19) Miller, S. T.; Xavier, K. B.; Campagna, S. R.; Taga, M. E.; Semmelhack, M. F.; Bassler, B. L.; Hughson, F. M. Salmonella Typhimurium Recognizes a Chemically Distinct Form of the Bacterial Quorum-Sensing Signal AI-2. *Mol. Cell* **2004**, *15* (5), 677–687.
(20) Schauder, S.; Shokat, K.; Surette, M. G.; Bassler, B. L. The LuxS Family of Bacterial Autoinducers: Biosynthesis of a Novel Quorum-Sensing Signal Molecule. *Mol. Microbiol.* **2001**, *41* (2), 463–476.
(21) Taga, M. E.; Semmelhack, J. L.; Bassler, B. L. The LuxS-Dependent Autoinducer AI-2 Controls the Expression of an ABC Transporter That Functions in AI-2 Uptake in Salmonella Typhimurium. *Mol. Microbiol.* **2001**, *42* (3), 777–793.
(22) Taga, M. E.; Miller, S. T.; Bassler, B. L. Lsr-Mediated Transport and Processing of AI-2 in Salmonella Typhimurium: Transport and Processing of AI-2. *Mol. Microbiol.* **2003**, *50* (4), 1411–1427.
(23) Xavier, K. B.; Bassler, B. L. Regulation of Uptake and Processing of the Quorum-Sensing Autoinducer AI-2 in Escherichia Coli. *J. Bacteriol.* **2005**, *187* (1), 238–248.
(24) Zhu, J.; Hixon, M. S.; Globisch, D.; Kaufmann, G. F.; Janda, K. D. Mechanistic Insights into the LsrK Kinase Required for Autoinducer-2 Quorum Sensing Activation. *J. Am. Chem. Soc.* **2013**, *135* (21), 7827–7830.
(25) Marques, J. C.; Oh, I. K.; Ly, D. C.; Lamosa, P.; Ventura, M. R.; Miller, S. T.; Xavier, K. B. LsrF, a Coenzyme A-Dependent Thiolase, Catalyzes the Terminal Step in Processing the Quorum Sensing Signal Autoinducer-2. *Proc. Natl. Acad. Sci. U. S. A.* **2014**, *111* (39), 14235–14240.
(26) Diaz, Z.; Xavier, K. B.; Miller, S. T. The Crystal Structure of the Escherichia Coli Autoinducer-2 Processing Protein LsrF. *PLoS One* **2009**, *4* (8), e6820.
(27) Pereira, C. S.; de Regt, A. K.; Brito, P. H.; Miller, S. T.; Xavier, K. B. Identification of Functional LsrB-Like Autoinducer-2 Receptors. *J. Bacteriol.* **2009**, *191* (22), 6975–6987.
(28) Chen, Y.-R.; Hartman, F. C.; Lu, T.-Y. S.; Larimer, F. W. D-Ribulose-5-Phosphate 3-Epimerase: Cloning and Heterologous Expression of the Spinach Gene, and Purification and Characterization of the Recombinant Enzyme. *Plant Physiol.* **1998**, *118* (1), 199–207.
(29) Karmali, A.; Drake, A. F.; Spencer, N. Purification, Properties and Assay of D-Ribulose 5-Phosphate 3-Epimerase from Human Erythrocytes. *Biochem. J.* **1983**, *211* (3), 617–623.
(30) Tanner, S. *Investigations of LsrG from E. Coli and LsrE from S. Typhimurium*; Swarthmore College: Swarthmore, PA, 2016: Swarthmore College: Swarthmore, PA, 2016.

(31) Smith, B. C.; Hallows, W. C.; Denu, J. M. A Continuous Microplate Assay for Sirtuins and Nicotinamide Producing Enzymes. *Anal. Biochem.* **2009**, *394* (1), 101–109.
(32) Lebendiker, M.; Danieli, T. Production of Prone-to-Aggregate Proteins. *FEBS Lett.* **2014**, *588* (2), 236–246.
(33) Kelley, L. A.; Mezulis, S.; Yates, C. M.; Wass, M. N.; Sternberg, M. J. E. The Phyre2 Web Portal for Protein Modeling, Prediction and Analysis. *Nat. Protoc.* **2015**, *10* (6), 845–858.
(34) Kapust, R. B.; Waugh, D. S. Escherichia Coli Maltose-Binding Protein Is Uncommonly Effective at Promoting the Solubility of Polypeptides to Which It Is Fused. *Protein Sci. Publ. Protein Soc.* **1999**, *8* (8), 1668–1674.
(35) Artimo, P.; Jonnalagedda, M.; Arnold, K.; Baratin, D.; Csardi, G.; de Castro, E.; Duvaud, S.; Flegel, V.; Fortier, A.; Gasteiger, E.; et al. ExPASy: SIB Bioinformatics Resource Portal. *Nucleic Acids Res.* **2012**, *40* (Web Server issue), W597–W603.
(36) Kågedal, L.; Engström, B.; Elelgren, H.; Lieber, A.-K.; Lundström, H.; Sköld, A.; Schenning, M. Chemical, Physical and Chromatographic Properties of Superdex 75 Prep Grade and Superdex 200 Prep Grade Gel Filtration Media. *J. Chromatogr. A* **1991**, *537*, 17–32.
(37) Hong, P.; Koza, S.; Bouvier, E. S. P. Size-Exclusion Chromatography for the Analysis of Protein Biotherapeutics and Their Aggregates. *J. Liq. Chromatogr. Relat. Technol.* **2012**, *35* (20), 2923–2950.
(38) Smyth, D. R.; Mrozkiewicz, M. K.; McGrath, W. J.; Listwan, P.; Kobe, B. Crystal Structures of Fusion Proteins with Large-Affinity Tags. *Protein Sci. Publ. Protein Soc.* **2003**, *12* (7), 1313–1322.
(39) Nguyen, H. H.; Park, J.; Kang, S.; Kim, M. Surface Plasmon Resonance: A Versatile Technique for Biosensor Applications. *Sensors* **2015**, *15* (5), 10481–10510.
(40) Freyer, M. W.; Lewis, E. A. Isothermal Titration Calorimetry: Experimental Design, Data Analysis, and Probing Macromolecule/Ligand Binding and Kinetic Interactions. In *Methods in Cell Biology*; Elsevier, 2008; Vol. 84, pp 79–113.
(41) Kasal, M. *Investigation of AI-2 Binding to the Quorum Sensing Receptor LsrB*; Swarthmore College: Swarthmore, PA, 2016: Swarthmore College: Swarthmore, PA, 2016.
(42) Kanehisa, M.; Goto, S. KEGG: Kyoto Encyclopedia of Genes and Genomes. *Nucleic Acids Res.* **2000**, *28* (1), 27–30.
(43) Sato, Y.; Nakaya, A.; Shiraishi, K.; Kawashima, S.; Goto, S.; Kanehisa, M. Ssdb: Sequence Similarity Database in Kegg. *Genome Inform.* **2001**, *12*, 230–231.
(44) Taga, M. E.; Xavier, K. B. Methods for Analysis of Bacterial Autoinducer-2 Production. In *Current Protocols in Microbiology*; Coico, R., McBride, A., Quarles, J. M., Stevenson, B., Taylor, R. K., Eds.; John Wiley & Sons, Inc.: Hoboken, NJ, USA, 2011; pp 1C.1.1-1C.1.15.
(45) Watanabe, K.; Nagao, N.; Yamamoto, S.; Toda, T.; Kurosawa, N. Thermobacillus Composti Sp. Nov., a Moderately Thermophilic Bacterium Isolated from a Composting Reactor. *Int. J. Syst. Evol. Microbiol.* **2007**, *57* (7), 1473–1477.
(46) Daniel, R. M.; Dines, M.; Petach, H. H. The Denaturation and Degradation of Stable Enzymes at High Temperatures. *Biochem. J.* **1996**, *317* (Pt 1), 1–11.

(47) Kirsch, P. D.; Ekerdt, J. G. KaleidaGraph: Graphing and Data Analysis. Version 3.5 for Windows Synergy Software, 2457 Perkiomen Ave., Reading, PA 19606-2049. Www.Synergy.Com. $155.00. *J. Am. Chem. Soc.* **2000**, *122* (47), 11755–11755.
(48) Bian, X.; Lockless, S. W. Preparation To Minimize Buffer Mismatch in Isothermal Titration Calorimetry Experiments. *Anal. Chem.* **2016**, *88* (10), 5549–5553.
(49) Ascenso, O. S.; Marques, J. C.; Santos, A. R.; Xavier, K. B.; Rita Ventura, M.; Maycock, C. D. An Efficient Synthesis of the Precursor of AI-2, the Signalling Molecule for Inter-Species Quorum Sensing. *Bioorg. Med. Chem.* **2011**, *19* (3), 1236–1241.
(50) Rajarathnam, K.; Rösgen, J. Isothermal Titration Calorimetry of Membrane Proteins – Progress and Challenges. *Biochim. Biophys. Acta* **2014**, *1838* (1).
(51) Turnbull, W. B.; Daranas, A. H. On the Value of *c* : Can Low Affinity Systems Be Studied by Isothermal Titration Calorimetry? *J. Am. Chem. Soc.* **2003**, *125* (48), 14859–14866.
(52) Carolan, C. G.; Lamzin, V. S. Automated Identification of Crystallographic Ligands Using Sparse-Density Representations. *Acta Crystallogr. D Biol. Crystallogr.* **2014**, *70* (Pt 7), 1844–1853.
(53) Kavanaugh, J. S.; Gakhar, L.; Horswill, A. R. The Structure of LsrB from Yersinia Pestis Complexed with Autoinducer-2. *Acta Crystallograph. Sect. F Struct. Biol. Cryst. Commun.* **2011**, *67* (Pt 12), 1501–1505.
(54) Stols, L.; Gu, M.; Dieckman, L.; Raffen, R.; Collart, F. R.; Donnelly, M. I. A New Vector for High-Throughput, Ligation-Independent Cloning Encoding a Tobacco Etch Virus Protease Cleavage Site. *Protein Expr. Purif.* **2002**, *25* (1), 8–15.
(55) Slabinski, L.; Jaroszewski, L.; Rychlewski, L.; Wilson, I. A.; Lesley, S. A.; Godzik, A. XtalPred: A Web Server for Prediction of Protein Crystallizability. *Bioinformatics* **2007**, *23* (24), 3403–3405.
(56) Wahab, M. F.; Anderson, J. K.; Abdelrady, M.; Lucy, C. A. Peak Distortion Effects in Analytical Ion Chromatography. *Anal. Chem.* **2014**, *86* (1), 559–566.
(57) Adams, P. D.; Afonine, P. V.; Bunkóczi, G.; Chen, V. B.; Davis, I. W.; Echols, N.; Headd, J. J.; Hung, L.-W.; Kapral, G. J.; Grosse-Kunstleve, R. W.; et al. *PHENIX* : A Comprehensive Python-Based System for Macromolecular Structure Solution. *Acta Crystallogr. D Biol. Crystallogr.* **2010**, *66* (2), 213–221.
(58) Helliwell, J. R. Macromolecular Crystal Twinning, Lattice Disorders and Multiple Crystals1. *Crystallogr. Rev.* **2008**, *14* (3), 189–250.
(59) Hendrickson, W. A. Anomalous Diffraction in Crystallographic Phase Evaluation. *Q. Rev. Biophys.* **2014**, *47* (1), 49–93.
(60) Bergfors, T. Succeeding with Seeding: Some Practical Advice. In Evolving Methods for Macromolecular Crystallography; NATO Science Series; Springer, Dordrecht, 2007; pp 1–10.

Supplemental Information

Table S1. List of primers used in the generation of truncations for both *Salmonella enterica* ser. *Typhimurium* LsrE and *Thermobacillus composti* LsrB.

Primer Name	5' → 3' Forward Primer	5' → 3' Reverse Primer
LsrE Non-truncated Forward	CACCATGAACAGCCAGTTTGCC	pDEST-HisMBP
LsrE 7' Truncated Forward	CACCTTAACGCGCGAAGCAT	pDEST-HisMBP
LsrE 19' Truncated Forward	CACCTATCCGCTTAGTGTGGGTATTC	pDEST-HisMBP
LsrE Non-Truncated Reverse	TTATGCTGTGGAGGGTAAGAAAGTAGTATC	pDEST-HisMBP
LsrE 244' Truncated Reverse	TTAGGCAACCTTAAACATCGCCC	pDEST-HisMBP
LsrB Truncated Forward	TACTTCCAATCCAATGCACGGCATCCGGACCGGC	pLIC-Tr3a-HA
LsrB Truncated Forward Alternate	TACTTCCAATCCAATGCACGGCATCCGGACCG	pLIC- Tr3a -HA
LsrB Truncated Reverse	TTATCCACTTCCAATGTTATTATCAAAAATCATA CTGGTCCACATTATCCTTCG	pLIC- Tr3a -HA

Table S2. Protein parameters calculated by ExPASy. These parameters were used to visualize protein by SDS-PAGE, as well as calculate concentration and ion exchange parameters.

Construct Name	Concentration Correction Factor	Isoelectric Point	Molecular weight (kDa)
His-MBP-LsrE Truncation5	1.431	5.63	70
LsrE Truncation 5	1.182	5.87	27
T. composti His_6-LsrB	1.183	5.03	36
T. composti LsrB	1.239	4.71	33

Table S3. Statistics from the *Vibrio harveyi* bioluminescence assay as calculated by the Student' t-test with Bonferroni correction.

Group 1	Group 2	t-value	p-value
E. coli with Protease	E. coli with Proteinase K	0.2508	1
E. coli with Protease	E. coli without Protease	2.6227	1
E. coli with Protease	E. coli with Protease and Heat	10.9666	< .0001
E. coli with Protease	E. coli with Proteinase K and Heat	4.8968	0.0032
E. coli with Protease	E. coli with Heat	6.2561	< .0001
E. coli with Protease	T. composti LuxS- with Protease	37.1485	< .0001
E. coli with Protease	T. composti LuxS- with Proteinase K	37.1446	< .0001
E. coli with Protease	T. composti LuxS- without Protease	37.1506	< .0001
E. coli with Protease	T. composti LuxS- with Protease and Heat	37.1507	< .0001
E. coli with Protease	T. composti LuxS- with Proteinase K and Heat	37.1304	< .0001
E. coli with Protease	T. composti LuxS- with Heat	37.1274	< .0001
E. coli with Protease	Old T. composti LuxS+ with Protease	27.29	< .0001
E. coli with Protease	Old T. composti LuxS+ with Proteinase K	23.2283	< .0001
E. coli with Protease	Old T. composti LuxS+ without Protease	34.9161	< .0001
E. coli with Protease	Old T. composti LuxS+ with Protease and Heat	33.6448	< .0001
E. coli with Protease	Old T. composti LuxS+ with Proteinase K and Heat	32.6511	< .0001
E. coli with Protease	Old T. composti LuxS+ with Heat	36.6576	< .0001
E. coli with Protease	New T. composti LuxS+ with Protease	1.178	1
E. coli with Protease	New T. composti LuxS+ with Proteinase K	1.9412	1
E. coli with Protease	New T. composti LuxS+ without Protease	22.9369	< .0001
E. coli with Protease	New T. composti LuxS+ with Protease and Heat	2.7992	1
E. coli with Protease	New T. composti LuxS+ with Proteinase K and Heat	3.0453	1
E. coli with Protease	New T. composti LuxS+ with Heat	20.727	< .0001
E. coli with Proteinase K	E. coli without Protease	2.3719	1
E. coli with Proteinase K	E. coli with Protease and Heat	10.7158	< .0001
E. coli with Proteinase K	E. coli with Proteinase K and Heat	4.6459	0.0073
E. coli with Proteinase K	E. coli with Heat	6.0053	< .0001
E. coli with Proteinase K	T. composti LuxS- with Protease	36.8977	< .0001
E. coli with Proteinase K	T. composti LuxS- with Proteinase K	36.8938	< .0001
E. coli with Proteinase K	T. composti LuxS- without Protease	36.8998	< .0001
E. coli with Proteinase K	T. composti LuxS- with Protease and Heat	36.8999	< .0001
E. coli with Proteinase K	T. composti LuxS- with Proteinase K and Heat	36.8796	< .0001
E. coli with Proteinase K	T. composti LuxS- with Heat	36.8766	< .0001
E. coli with Proteinase K	Old T. composti LuxS+ with Protease	27.0392	< .0001
E. coli with Proteinase K	Old T. composti LuxS+ with Proteinase K	22.9775	< .0001
E. coli with Proteinase K	Old T. composti LuxS+ without Protease	34.6653	< .0001
E. coli with Proteinase K	Old T. composti LuxS+ with Protease and Heat	33.394	< .0001
E. coli with Proteinase K	Old T. composti LuxS+ with Proteinase K and Heat	32.4003	< .0001
E. coli with Proteinase K	Old T. composti LuxS+ with Heat	36.4068	< .0001

Table S3. Continued.

Group 1	Group 2	t-value	p-value
E. coli with Proteinase K	New T. composti LuxS+ with Protease	0.9272	1
E. coli with Proteinase K	New T. composti LuxS+ with Proteinase K	2.192	1
E. coli with Proteinase K	New T. composti LuxS+ without Protease	22.686	< .0001
E. coli with Proteinase K	New T. composti LuxS+ with Protease and Heat	2.5484	1
E. coli with Proteinase K	New T. composti LuxS+ with Proteinase K and Heat	3.2961	0.5103
E. coli with Proteinase K	New T. composti LuxS+ with Heat	20.4762	< .0001
E. coli without Protease	E. coli with Protease and Heat	8.3439	< .0001
E. coli without Protease	E. coli with Proteinase K and Heat	2.2741	1
E. coli without Protease	E. coli with Heat	3.6334	0.1876
E. coli without Protease	T. composti LuxS- with Protease	34.5258	< .0001
E. coli without Protease	T. composti LuxS- with Proteinase K	34.5219	< .0001
E. coli without Protease	T. composti LuxS- without Protease	34.5279	< .0001
E. coli without Protease	T. composti LuxS- with Protease and Heat	34.528	< .0001
E. coli without Protease	T. composti LuxS- with Proteinase K and Heat	34.5077	< .0001
E. coli without Protease	T. composti LuxS- with Heat	34.5048	< .0001
E. coli without Protease	Old T. composti LuxS+ with Protease	24.6674	< .0001
E. coli without Protease	Old T. composti LuxS+ with Proteinase K	20.6056	< .0001
E. coli without Protease	Old T. composti LuxS+ without Protease	32.2934	< .0001
E. coli without Protease	Old T. composti LuxS+ with Protease and Heat	31.0221	< .0001
E. coli without Protease	Old T. composti LuxS+ with Proteinase K and Heat	30.0284	< .0001
E. coli without Protease	Old T. composti LuxS+ with Heat	34.0349	< .0001
E. coli without Protease	New T. composti LuxS+ with Protease	1.4447	1
E. coli without Protease	New T. composti LuxS+ with Proteinase K	4.5639	0.0097
E. coli without Protease	New T. composti LuxS+ without Protease	20.3142	< .0001
E. coli without Protease	New T. composti LuxS+ with Protease and Heat	0.1765	1
E. coli without Protease	New T. composti LuxS+ with Proteinase K and Heat	5.668	0.0002
E. coli without Protease	New T. composti LuxS+ with Heat	18.1044	< .0001
E. coli with Protease and Heat	E. coli with Proteinase K and Heat	6.0698	< .0001
E. coli with Protease and Heat	E. coli with Heat	4.7105	0.0059
E. coli with Protease and Heat	T. composti LuxS- with Protease	26.1819	< .0001
E. coli with Protease and Heat	T. composti LuxS- with Proteinase K	26.178	< .0001
E. coli with Protease and Heat	T. composti LuxS- without Protease	26.184	< .0001
E. coli with Protease and Heat	T. composti LuxS- with Protease and Heat	26.1841	< .0001
E. coli with Protease and Heat	T. composti LuxS- with Proteinase K and Heat	26.1638	< .0001
E. coli with Protease and Heat	T. composti LuxS- with Heat	26.1609	< .0001
E. coli with Protease and Heat	Old T. composti LuxS+ with Protease	16.3235	< .0001
E. coli with Protease and Heat	Old T. composti LuxS+ with Proteinase K	12.2617	< .0001
E. coli with Protease and Heat	Old T. composti LuxS+ without Protease	23.9495	< .0001
E. coli with Protease and Heat	Old T. composti LuxS+ with Protease and Heat	22.6782	< .0001
E. coli with Protease and Heat	Old T. composti LuxS+ with Proteinase K and Heat	21.6845	< .0001

Table S3. Continued.

Group 1	Group 2	t-value	p-value
E. coli with Protease and Heat	Old T. composti LuxS+ with Heat	25.691	< .0001
E. coli with Protease and Heat	New T. composti LuxS+ with Protease	9.7886	< .0001
E. coli with Protease and Heat	New T. composti LuxS+ with Proteinase K	12.9078	< .0001
E. coli with Protease and Heat	New T. composti LuxS+ without Protease	11.9703	< .0001
E. coli with Protease and Heat	New T. composti LuxS+ with Protease and Heat	8.1674	< .0001
E. coli with Protease and Heat	New T. composti LuxS+ with Proteinase K and Heat	14.0119	< .0001
E. coli with Protease and Heat	New T. composti LuxS+ with Heat	9.7605	< .0001
E. coli with Proteinase K and Heat	E. coli with Heat	1.3593	1
E. coli with Proteinase K and Heat	T. composti LuxS- with Protease	32.2518	< .0001
E. coli with Proteinase K and Heat	T. composti LuxS- with Proteinase K	32.2479	< .0001
E. coli with Proteinase K and Heat	T. composti LuxS- without Protease	32.2539	< .0001
E. coli with Proteinase K and Heat	T. composti LuxS- with Protease and Heat	32.254	< .0001
E. coli with Proteinase K and Heat	T. composti LuxS- with Proteinase K and Heat	32.2336	< .0001
E. coli with Proteinase K and Heat	T. composti LuxS- with Heat	32.2307	< .0001
E. coli with Proteinase K and Heat	Old T. composti LuxS+ with Protease	22.3933	< .0001
E. coli with Proteinase K and Heat	Old T. composti LuxS+ with Proteinase K	18.3315	< .0001
E. coli with Proteinase K and Heat	Old T. composti LuxS+ without Protease	30.0193	< .0001
E. coli with Proteinase K and Heat	Old T. composti LuxS+ with Protease and Heat	28.748	< .0001
E. coli with Proteinase K and Heat	Old T. composti LuxS+ with Proteinase K and Heat	27.7543	< .0001
E. coli with Proteinase K and Heat	Old T. composti LuxS+ with Heat	31.7608	< .0001
E. coli with Proteinase K and Heat	New T. composti LuxS+ with Protease	3.7187	0.1446
E. coli with Proteinase K and Heat	New T. composti LuxS+ with Proteinase K	6.8379	< .0001
E. coli with Proteinase K and Heat	New T. composti LuxS+ without Protease	18.0401	< .0001
E. coli with Proteinase K and Heat	New T. composti LuxS+ with Protease and Heat	2.0975	1
E. coli with Proteinase K and Heat	New T. composti LuxS+ with Proteinase K and Heat	7.9421	< .0001
E. coli with Proteinase K and Heat	New T. composti LuxS+ with Heat	15.8303	< .0001
E. coli with Heat	T. composti LuxS- with Protease	30.8924	< .0001
E. coli with Heat	T. composti LuxS- with Proteinase K	30.8885	< .0001
E. coli with Heat	T. composti LuxS- without Protease	30.8945	< .0001
E. coli with Heat	T. composti LuxS- with Protease and Heat	30.8946	< .0001
E. coli with Heat	T. composti LuxS- with Proteinase K and Heat	30.8743	< .0001
E. coli with Heat	T. composti LuxS- with Heat	30.8713	< .0001
E. coli with Heat	Old T. composti LuxS+ with Protease	21.034	< .0001
E. coli with Heat	Old T. composti LuxS+ with Proteinase K	16.9722	< .0001
E. coli with Heat	Old T. composti LuxS+ without Protease	28.66	< .0001
E. coli with Heat	Old T. composti LuxS+ with Protease and Heat	27.3887	< .0001
E. coli with Heat	Old T. composti LuxS+ with Proteinase K and Heat	26.395	< .0001
E. coli with Heat	Old T. composti LuxS+ with Heat	30.4015	< .0001
E. coli with Heat	New T. composti LuxS+ with Protease	5.0781	0.0017
E. coli with Heat	New T. composti LuxS+ with Proteinase K	8.1973	< .0001

Table S3. Continued.

Group 1	Group 2	t-value	p-value
E. coli with Heat	New T. composti LuxS+ without Protease	16.6808	< .0001
E. coli with Heat	New T. composti LuxS+ with Protease and Heat	3.4569	0.3185
E. coli with Heat	New T. composti LuxS+ with Proteinase K and Heat	9.3014	< .0001
E. coli with Heat	New T. composti LuxS+ with Heat	14.471	< .0001
T. composti LuxS- with Protease	T. composti LuxS- with Proteinase K	0.0039	1
T. composti LuxS- with Protease	T. composti LuxS- without Protease	0.0021	1
T. composti LuxS- with Protease	T. composti LuxS- with Protease and Heat	0.0022	1
T. composti LuxS- with Protease	T. composti LuxS- with Proteinase K and Heat	0.0181	1
T. composti LuxS- with Protease	T. composti LuxS- with Heat	0.0211	1
T. composti LuxS- with Protease	Old T. composti LuxS+ with Protease	9.8585	< .0001
T. composti LuxS- with Protease	Old T. composti LuxS+ with Proteinase K	13.9202	< .0001
T. composti LuxS- with Protease	Old T. composti LuxS+ without Protease	2.2324	1
T. composti LuxS- with Protease	Old T. composti LuxS+ with Protease and Heat	3.5038	0.2771
T. composti LuxS- with Protease	Old T. composti LuxS+ with Proteinase K and Heat	4.4974	0.012
T. composti LuxS- with Protease	Old T. composti LuxS+ with Heat	0.491	1
T. composti LuxS- with Protease	New T. composti LuxS+ with Protease	35.9705	< .0001
T. composti LuxS- with Protease	New T. composti LuxS+ with Proteinase K	39.0897	< .0001
T. composti LuxS- with Protease	New T. composti LuxS+ without Protease	14.2117	< .0001
T. composti LuxS- with Protease	New T. composti LuxS+ with Protease and Heat	34.3493	< .0001
T. composti LuxS- with Protease	New T. composti LuxS+ with Proteinase K and Heat	40.1938	< .0001
T. composti LuxS- with Protease	New T. composti LuxS+ with Heat	16.4215	< .0001
. composti LuxS- with Proteinase K	T. composti LuxS- without Protease	0.006	1
. composti LuxS- with Proteinase K	T. composti LuxS- with Protease and Heat	0.0061	1
. composti LuxS- with Proteinase K	T. composti LuxS- with Proteinase K and Heat	0.0142	1
. composti LuxS- with Proteinase K	T. composti LuxS- with Heat	0.0172	1
. composti LuxS- with Proteinase K	Old T. composti LuxS+ with Protease	9.8546	< .0001
. composti LuxS- with Proteinase K	Old T. composti LuxS+ with Proteinase K	13.9163	< .0001
. composti LuxS- with Proteinase K	Old T. composti LuxS+ without Protease	2.2285	1
. composti LuxS- with Proteinase K	Old T. composti LuxS+ with Protease and Heat	3.4998	0.2803
. composti LuxS- with Proteinase K	Old T. composti LuxS+ with Proteinase K and Heat	4.4935	0.0122
. composti LuxS- with Proteinase K	Old T. composti LuxS+ with Heat	0.487	1
. composti LuxS- with Proteinase K	New T. composti LuxS+ with Protease	35.9666	< .0001
. composti LuxS- with Proteinase K	New T. composti LuxS+ with Proteinase K	39.0858	< .0001
. composti LuxS- with Proteinase K	New T. composti LuxS+ without Protease	14.2078	< .0001
. composti LuxS- with Proteinase K	New T. composti LuxS+ with Protease and Heat	34.3454	< .0001
. composti LuxS- with Proteinase K	New T. composti LuxS+ with Proteinase K and Heat	40.1899	< .0001
. composti LuxS- with Proteinase K	New T. composti LuxS+ with Heat	16.4176	< .0001
T. composti LuxS- without Protease	T. composti LuxS- with Protease and Heat	0.0001	1
T. composti LuxS- without Protease	T. composti LuxS- with Proteinase K and Heat	0.0202	1
T. composti LuxS- without Protease	T. composti LuxS- with Heat	0.0232	1

Table S3. Continued.

Group 1	Group 2	t-value	p-value
T. composti LuxS- without Protease	Old T. composti LuxS+ with Protease	9.8606	< .0001
T. composti LuxS- without Protease	Old T. composti LuxS+ with Proteinase K	13.9223	< .0001
T. composti LuxS- without Protease	Old T. composti LuxS+ without Protease	2.2345	1
T. composti LuxS- without Protease	Old T. composti LuxS+ with Protease and Heat	3.5058	0.2754
T. composti LuxS- without Protease	Old T. composti LuxS+ with Proteinase K and Heat	4.4995	0.0119
T. composti LuxS- without Protease	Old T. composti LuxS+ with Heat	0.493	1
T. composti LuxS- without Protease	New T. composti LuxS+ with Protease	35.9726	< .0001
T. composti LuxS- without Protease	New T. composti LuxS+ with Proteinase K	39.0918	< .0001
T. composti LuxS- without Protease	New T. composti LuxS+ without Protease	14.2138	< .0001
T. composti LuxS- without Protease	New T. composti LuxS+ with Protease and Heat	34.3514	< .0001
T. composti LuxS- without Protease	New T. composti LuxS+ with Proteinase K and Heat	40.1959	< .0001
T. composti LuxS- without Protease	New T. composti LuxS+ with Heat	16.4236	< .0001
T. composti LuxS- with Protease and Heat	T. composti LuxS- with Proteinase K and Heat	0.0203	1
T. composti LuxS- with Protease and Heat	T. composti LuxS- with Heat	0.0233	1
T. composti LuxS- with Protease and Heat	Old T. composti LuxS+ with Protease	9.8607	< .0001
T. composti LuxS- with Protease and Heat	Old T. composti LuxS+ with Proteinase K	13.9224	< .0001
T. composti LuxS- with Protease and Heat	Old T. composti LuxS+ without Protease	2.2346	1
T. composti LuxS- with Protease and Heat	Old T. composti LuxS+ with Protease and Heat	3.5059	0.2753
T. composti LuxS- with Protease and Heat	Old T. composti LuxS+ with Proteinase K and Heat	4.4996	0.0119
T. composti LuxS- with Protease and Heat	Old T. composti LuxS+ with Heat	0.4932	1
T. composti LuxS- with Protease and Heat	New T. composti LuxS+ with Protease	35.9727	< .0001
T. composti LuxS- with Protease and Heat	New T. composti LuxS+ with Proteinase K	39.0919	< .0001
T. composti LuxS- with Protease and Heat	New T. composti LuxS+ without Protease	14.2139	< .0001
T. composti LuxS- with Protease and Heat	New T. composti LuxS+ with Protease and Heat	34.3515	< .0001
T. composti LuxS- with Protease and Heat	New T. composti LuxS+ with Proteinase K and Heat	40.196	< .0001
T. composti LuxS- with Protease and Heat	New T. composti LuxS+ with Heat	16.4237	< .0001
T. composti LuxS- with Proteinase K and Heat	T. composti LuxS- with Heat	0.003	1
T. composti LuxS- with Proteinase K and Heat	Old T. composti LuxS+ with Protease	9.8403	< .0001
T. composti LuxS- with Proteinase K and Heat	Old T. composti LuxS+ with Proteinase K	13.9021	< .0001
T. composti LuxS- with Proteinase K and Heat	Old T. composti LuxS+ without Protease	2.2143	1
T. composti LuxS- with Proteinase K and Heat	Old T. composti LuxS+ with Protease and Heat	3.4856	0.2925
T. composti LuxS- with Proteinase K and Heat	Old T. composti LuxS+ with Proteinase K and Heat	4.4793	0.0128
T. composti LuxS- with Proteinase K and Heat	Old T. composti LuxS+ with Heat	0.4728	1
T. composti LuxS- with Proteinase K and Heat	New T. composti LuxS+ with Protease	35.9524	< .0001
T. composti LuxS- with Proteinase K and Heat	New T. composti LuxS+ with Proteinase K	39.0716	< .0001
T. composti LuxS- with Proteinase K and Heat	New T. composti LuxS+ without Protease	14.1935	< .0001
T. composti LuxS- with Proteinase K and Heat	New T. composti LuxS+ with Protease and Heat	34.3312	< .0001
T. composti LuxS- with Proteinase K and Heat	New T. composti LuxS+ with Proteinase K and Heat	40.1757	< .0001
T. composti LuxS- with Proteinase K and Heat	New T. composti LuxS+ with Heat	16.4033	< .0001
T. composti LuxS- with Heat	Old T. composti LuxS+ with Protease	9.8374	< .0001

Table S3. Continued.

Group 1	Group 2	t-value	p-value
T. composti LuxS- with Heat	Old T. composti LuxS+ with Proteinase K	13.8991	< .0001
T. composti LuxS- with Heat	Old T. composti LuxS+ without Protease	2.2113	1
T. composti LuxS- with Heat	Old T. composti LuxS+ with Protease and Heat	3.4827	0.2951
T. composti LuxS- with Heat	Old T. composti LuxS+ with Proteinase K and Heat	4.4763	0.0129
T. composti LuxS- with Heat	Old T. composti LuxS+ with Heat	0.4699	1
T. composti LuxS- with Heat	New T. composti LuxS+ with Protease	35.9494	< .0001
T. composti LuxS- with Heat	New T. composti LuxS+ with Proteinase K	39.0686	< .0001
T. composti LuxS- with Heat	New T. composti LuxS+ without Protease	14.1906	< .0001
T. composti LuxS- with Heat	New T. composti LuxS+ with Protease and Heat	34.3282	< .0001
T. composti LuxS- with Heat	New T. composti LuxS+ with Proteinase K and Heat	40.1727	< .0001
T. composti LuxS- with Heat	New T. composti LuxS+ with Heat	16.4004	< .0001
Old T. composti LuxS+ with Protease	Old T. composti LuxS+ with Proteinase K	4.0618	0.0495
Old T. composti LuxS+ with Protease	Old T. composti LuxS+ without Protease	7.626	< .0001
Old T. composti LuxS+ with Protease	Old T. composti LuxS+ with Protease and Heat	6.3547	< .0001
Old T. composti LuxS+ with Protease	Old T. composti LuxS+ with Proteinase K and Heat	5.3611	0.0006
Old T. composti LuxS+ with Protease	Old T. composti LuxS+ with Heat	9.3675	< .0001
Old T. composti LuxS+ with Protease	New T. composti LuxS+ with Protease	26.112	< .0001
Old T. composti LuxS+ with Protease	New T. composti LuxS+ with Proteinase K	29.2312	< .0001
Old T. composti LuxS+ with Protease	New T. composti LuxS+ without Protease	4.3532	0.0193
Old T. composti LuxS+ with Protease	New T. composti LuxS+ with Protease and Heat	24.4908	< .0001
Old T. composti LuxS+ with Protease	New T. composti LuxS+ with Proteinase K and Heat	30.3353	< .0001
Old T. composti LuxS+ with Protease	New T. composti LuxS+ with Heat	6.563	< .0001
Old T. composti LuxS+ with Proteinase K	Old T. composti LuxS+ without Protease	11.6878	< .0001
Old T. composti LuxS+ with Proteinase K	Old T. composti LuxS+ with Protease and Heat	10.4165	< .0001
Old T. composti LuxS+ with Proteinase K	Old T. composti LuxS+ with Proteinase K and Heat	9.4228	< .0001
Old T. composti LuxS+ with Proteinase K	Old T. composti LuxS+ with Heat	13.4293	< .0001
Old T. composti LuxS+ with Proteinase K	New T. composti LuxS+ with Protease	22.0503	< .0001
Old T. composti LuxS+ with Proteinase K	New T. composti LuxS+ with Proteinase K	25.1695	< .0001
Old T. composti LuxS+ with Proteinase K	New T. composti LuxS+ without Protease	0.2914	1
Old T. composti LuxS+ with Proteinase K	New T. composti LuxS+ with Protease and Heat	20.4291	< .0001
Old T. composti LuxS+ with Proteinase K	New T. composti LuxS+ with Proteinase K and Heat	26.2736	< .0001
Old T. composti LuxS+ with Proteinase K	New T. composti LuxS+ with Heat	2.5012	1
Old T. composti LuxS+ without Protease	Old T. composti LuxS+ with Protease and Heat	1.2713	1
Old T. composti LuxS+ without Protease	Old T. composti LuxS+ with Proteinase K and Heat	2.265	1
Old T. composti LuxS+ without Protease	Old T. composti LuxS+ with Heat	1.7415	1
Old T. composti LuxS+ without Protease	New T. composti LuxS+ with Protease	33.7381	< .0001
Old T. composti LuxS+ without Protease	New T. composti LuxS+ with Proteinase K	36.8573	< .0001
Old T. composti LuxS+ without Protease	New T. composti LuxS+ without Protease	11.9792	< .0001
Old T. composti LuxS+ without Protease	New T. composti LuxS+ with Protease and Heat	32.1169	< .0001
Old T. composti LuxS+ without Protease	New T. composti LuxS+ with Proteinase K and Heat	37.9614	< .0001

Table S3. Continued.

Group 1	Group 2	t-value	p-value
Old T. composti LuxS+ without Protease	New T. composti LuxS+ with Heat	14.189	< .0001
Old T. composti LuxS+ with Protease and Heat	Old T. composti LuxS+ with Proteinase K and Heat	0.9937	1
Old T. composti LuxS+ with Protease and Heat	Old T. composti LuxS+ with Heat	3.0128	1
Old T. composti LuxS+ with Protease and Heat	New T. composti LuxS+ with Protease	32.4668	< .0001
Old T. composti LuxS+ with Protease and Heat	New T. composti LuxS+ with Proteinase K	35.586	< .0001
Old T. composti LuxS+ with Protease and Heat	New T. composti LuxS+ without Protease	10.7079	< .0001
Old T. composti LuxS+ with Protease and Heat	New T. composti LuxS+ with Protease and Heat	30.8456	< .0001
Old T. composti LuxS+ with Protease and Heat	New T. composti LuxS+ with Proteinase K and Heat	36.6901	< .0001
Old T. composti LuxS+ with Protease and Heat	New T. composti LuxS+ with Heat	12.9177	< .0001
Old T. composti LuxS+ with Proteinase K and Heat	Old T. composti LuxS+ with Heat	4.0065	0.059
Old T. composti LuxS+ with Proteinase K and Heat	New T. composti LuxS+ with Protease	31.4731	< .0001
Old T. composti LuxS+ with Proteinase K and Heat	New T. composti LuxS+ with Proteinase K	34.5923	< .0001
Old T. composti LuxS+ with Proteinase K and Heat	New T. composti LuxS+ without Protease	9.7142	< .0001
Old T. composti LuxS+ with Proteinase K and Heat	New T. composti LuxS+ with Protease and Heat	29.8519	< .0001
Old T. composti LuxS+ with Proteinase K and Heat	New T. composti LuxS+ with Proteinase K and Heat	35.6964	< .0001
Old T. composti LuxS+ with Proteinase K and Heat	New T. composti LuxS+ with Heat	11.9241	< .0001
Old T. composti LuxS+ with Heat	New T. composti LuxS+ with Protease	35.4796	< .0001
Old T. composti LuxS+ with Heat	New T. composti LuxS+ with Proteinase K	38.5988	< .0001
Old T. composti LuxS+ with Heat	New T. composti LuxS+ without Protease	13.7207	< .0001
Old T. composti LuxS+ with Heat	New T. composti LuxS+ with Protease and Heat	33.8584	< .0001
Old T. composti LuxS+ with Heat	New T. composti LuxS+ with Proteinase K and Heat	39.7029	< .0001
Old T. composti LuxS+ with Heat	New T. composti LuxS+ with Heat	15.9305	< .0001
New T. composti LuxS+ with Protease	New T. composti LuxS+ with Proteinase K	3.1192	0.8458
New T. composti LuxS+ with Protease	New T. composti LuxS+ without Protease	21.7588	< .0001
New T. composti LuxS+ with Protease	New T. composti LuxS+ with Protease and Heat	1.6212	1
New T. composti LuxS+ with Protease	New T. composti LuxS+ with Proteinase K and Heat	4.2233	0.0295
New T. composti LuxS+ with Protease	New T. composti LuxS+ with Heat	19.549	< .0001
New T. composti LuxS+ with Proteinase K	New T. composti LuxS+ without Protease	24.878	< .0001
New T. composti LuxS+ with Proteinase K	New T. composti LuxS+ with Protease and Heat	4.7404	0.0054
New T. composti LuxS+ with Proteinase K	New T. composti LuxS+ with Proteinase K and Heat	1.1041	1
New T. composti LuxS+ with Proteinase K	New T. composti LuxS+ with Heat	22.6682	< .0001
New T. composti LuxS+ without Protease	New T. composti LuxS+ with Protease and Heat	20.1376	< .0001
New T. composti LuxS+ without Protease	New T. composti LuxS+ with Proteinase K and Heat	25.9822	< .0001
New T. composti LuxS+ without Protease	New T. composti LuxS+ with Heat	2.2098	1
New T. composti LuxS+ with Protease and Heat	New T. composti LuxS+ with Proteinase K and Heat	5.8445	0.0001
New T. composti LuxS+ with Protease and Heat	New T. composti LuxS+ with Heat	17.9278	< .0001
New T. composti LuxS+ with Proteinase K and Heat	New T. composti LuxS+ with Heat	23.7724	< .0001

Table S4. Statistics from the *Vibrio harveyi* bioluminescence assay calculated by the Student's t-test with Bonferroni correction.

Group 1	Group 2	t-value	p-value
E. coli Protein	B. anthracis Protein	1.288	1
E. coli Protein	T. composti Protein	12.5521	< .0001
E. coli Protein	E. coli Flow Through	3.7656	0.0324
E. coli Protein	B. anthracis Flow Through	3.8261	0.0284
E. coli Protein	T. composti Flow Through	10.4637	< .0001
E. coli Protein	Blank	14.9755	< .0001
B. anthracis Protein	T. composti Protein	13.8401	< .0001
B. anthracis Protein	E. coli Flow Through	5.0536	0.0021
B. anthracis Protein	B. anthracis Flow Through	5.1141	0.0018
B. anthracis Protein	T. composti Flow Through	11.7517	< .0001
B. anthracis Protein	Blank	16.4628	< .0001
T. composti Protein	E. coli Flow Through	8.7864	< .0001
T. composti Protein	B. anthracis Flow Through	8.726	< .0001
T. composti Protein	T. composti Flow Through	2.0884	1
T. composti Protein	Blank	0.4816	1
E. coli Flow Through	B. anthracis Flow Through	0.0605	1
E. coli Flow Through	T. composti Flow Through	6.6981	< .0001
E. coli Flow Through	Blank	10.6273	< .0001
B. anthracis Flow Through	T. composti Flow Through	6.6376	< .0001
B. anthracis Flow Through	Blank	10.5575	< .0001
T. composti Flow Through	Blank	2.893	0.2123

Table S5. N-terminal truncated *Thermobacillus composti* LsrB crystallized to many various morphologies under a wide range of conditions.

Buffer	Additive 1	Additive 2	Crystal Form
HEPES pH 8.5	150mM Sodium chloride	40% PEG 3350	Long, chunky tubes
HEPES pH 7.5	150mM Sodium chloride	40% PEG 3350	Long, chunky rods
100mM BIS-TRIS pH 6.5	150mM Sodium chloride	40% PEG 3350	Bulky rock-like crystals
100mM Tris pH 8.0	-	28% PEG 4000	Small crystal showers
100mM Sodium malonate pH 8.0	100mM Tris pH 8.0	30% PEG 1000	Needles
200mM Ammonium citrate tribasic pH 7.0	100mM Imidazole pH 7.0	20% PEG MME 2000	Needles
100mM Tris pH 8.0	2% 1,4-Dioxone	15% PEG 3350	Rock-like
100mM HEPES pH 7.5	200mM Sodium phosphate monobasic	200mM Potassium phosphate monobasic	Needles
100mM HEPES pH 7.5	200mM Calcium chloride dihydrate	28% PEG 400	Rock-like, soft edges
100mM HEPES pH 8.5	200mM Calcium chloride dihydrate	28% PEG 400	Rock-like, soft edges